Journal of Inflammation Research

Dovepress
open access to scientific and medical research

Open Access Full Text Article

ORIGINAL RESEARCH

Antimicrobial Activity of *Brassica rapa* L. Flowers Extract on Gastrointestinal Tract Infections and Antiulcer Potential Against Indomethacin-Induced Gastric Ulcer in Rats Supported by Metabolomics Profiling

Badriyah Alotaibi[1,*]
Fatma Alzahraa Mokhtar[2,*]
Thanaa A El-Masry[3]
Engy Elekhnawy[4]
Sally A Mostafa[5]
Dalia H Abdelkader[6]
Mohamed E Elharty[7]
Asmaa Saleh[1,8]
Walaa A Negm[9]

[1]Department of Pharmaceutical Sciences, College of Pharmacy, Princess Nourah Bint Abdulrahman University, Riyadh, 84428, Saudi Arabia; [2]Department of Pharmacognosy, Faculty of Pharmacy, ALsalam University, Al Gharbiyah, Egypt; [3]Department of Pharmacology and Toxicology, Faculty of Pharmacy, Tanta University, Tanta, 31111, Egypt; [4]Pharmaceutical Microbiology Department, Faculty of Pharmacy, Tanta University, Tanta, 31111, Egypt; [5]Department of Medical Biochemistry and Molecular Biology, Faculty of Medicine, Mansoura University, Mansoura, 35511, Egypt; [6]Department of Pharmaceutical Technology, Faculty of Pharmacy, Tanta University, Tanta, 31111, Egypt; [7]Study Master in Pharmaceutical Science at the Institute of Research and Environmental Studies, El Sadat City, Egypt; [8]Department of Biochemistry, Faculty of Pharmacy, Al Azhar University, Cairo, Egypt; [9]Department of Pharmacognosy, Faculty of Pharmacy, Tanta University, Tanta, 31111, Egypt

*These authors contributed equally to this work

Correspondence: Walaa A Negm
Department of Pharmacognosy, Faculty of Pharmacy, Tanta University, Tanta, 31111, Egypt
Tel +20403336007
Fax +20403335466
Email walaa.negm@pharm.tanta.edu.eg

Introduction: The gastrointestinal tract (GIT) is vulnerable to various diseases. In this study, we explored the therapeutic effects of *Brassica rapa* flower extract (BRFE) on GIT diseases.

Methods: Liquid chromatography–electrospray ionization–tandem mass spectrometry (LC-ESI-MS/MS) was used for phytochemical identification of the compounds in BRFE. The antibacterial activity of BRFE was investigated, and its impact on the bacterial outer and inner membrane permeability and membrane depolarization (using flow cytometry) was studied. In addition, the immunomodulatory activity of BRFE was investigated in vitro on lipopolysaccharide (LPS)-stimulated peripheral blood mononuclear cells (PBMCs) using quantitative reverse transcription polymerase chain reaction (qRT-PCR). Furthermore, the anti-inflammatory activity of BRFE was investigated by histopathological examination and qRT-PCR on indomethacin-induced gastric ulcers in rats.

Results and Discussion: LC-ESI-MS/MS phytochemically identified 57 compounds in BRFE for the first time. BRFE displayed antibacterial activity against bacteria that cause GIT infections, with increasing outer and inner membrane permeability. However, membrane depolarization was unaffected. BRFE also exhibited immunomodulatory activity in LPS-stimulated PBMCs by attenuating the upregulation of cyclooxygenase 2 (COX-2), inducible nitric oxide synthase (iNOS), interleukin (IL)-6, tumor necrosis factor-alpha (TNF-α), and nuclear factor kappa B (NF-κB) gene expression compared with untreated LPS-stimulated PBMCs. In addition, BRFE exhibited anti-inflammatory activity required for maintaining gastric mucosa homeostasis by decreasing neutrophil infiltration with subsequent myeloperoxidase production, in addition to an increase in glutathione peroxidase (GPx) activity. Histopathological findings presented the gastroprotective effects of BRFE, as a relatively normal stomach mucosa was found in treated rats. In addition, BRFE modulated the expression of genes encoding IL-10, NF-κB, GPx, and myeloperoxidase (MPO).

Conclusion: BRFE can be a promising source of therapeutic agents for treatment of GIT diseases.

Keywords: antioxidant activity, flow cytometry, GIT diseases, immunomodulatory activity, LC-MS/MS, qRT-PCR

Received: 25 October 2021
Accepted: 9 December 2021
Published: 29 December 2021

Introduction

Various plants contain many chemical compounds with wide structural diversity and good biological activity against different diseases.[1] Therefore, many scientists have focused their research on elucidation of the biological activity of different plant extracts to find new alternative therapeutic agents against various diseases. Gastrointestinal tract (GIT) diseases are any disorders in the digestive tract that extends from the oral cavity to the rectum. GIT diseases, unfortunately, have a relatively high prevalence worldwide.[2] Many drugs currently available for treatment of GIT diseases have disadvantages of low efficacy or high rates of side effects. Hence, many studies have investigated the potential therapeutic activity of different plants in GIT diseases.[3]

Brassica rapa L. (turnip; family Cruciferae)) is one of the first vegetables to be cultivated worldwide. Due to its nutritional characteristics, it is a popular crop for its edible components, including leaves, roots, and flowers, which are consumed in large amounts. *B. rapa* L. has been used for centuries to cure a number of disorders, including hepatitis, jaundice, diabetes, sore throat, constipation, and cholecystitis. In addition, it is used for lung protection and nephroprotection in Unani and Arab traditional medicine.[4–7]

B. rapa L. is reported to have a variety of secondary metabolites, such as glucosinolates, isothiocyanates, flavonoids, phenylpropanoids, sulfur-containing compounds, phenolics, indoles, and carbohydrates.[8–12] Its reproductive organs have the largest quantity of glucosinolates and nitrogen-containing chemicals, whereas volatile substances (terpenes and isoprenoids) are prevalent in seedlings and decrease with development. Progoitrin, gluconapoleiferin, gluconapin, 4-hydroxyglucobrassicin, glucobrassicanapin, glucobrassicin, gluconasturtiin, and neoglucobrassicin are the most prominent glucosinolates.[13] *B. rapa* L. greens and tops contain flavonoids, primarily quercetin, kaempferol, and isorhamnetin derivatives.[14] These major, active constituents of *B. rapa* L. show diverse bioactivities, including antioxidant, hepatoprotective, anticancer, antimicrobial, antidiabetic, nephroprotective, cardioprotective, hypolipidemic, analgesic, and anti-inflammatory effects.[5,15–17]

To date, different plant extracts have been established as prospective therapeutic agents for the treatment of different GIT diseases. In this study, we evaluated the potential antimicrobial activity of *B. rapa* flower extract (BRFE) on the bacteria that cause GIT infections. Additionally, previous studies have shown the anti-inflammatory and gastroprotective effects of some *Brassica* species,[18,19] which motivated us to conduct in vivo anti–gastric ulcer studies on BRFE. Moreover, we also investigated BRFE's in vitro immunomodulatory activity and explored the phytochemical profiling of BRFE's secondary metabolites.

Materials and Methods

Preparation of BRFE

B. rapa L. specimens were gathered from Al Keram Farms, El-Beheira Governorate, Egypt, in February 2021. The plant was recognized by Dr. Wafaa Amer at the Plant Taxonomy Department, Faculty of Science, Cairo University, Egypt. A voucher sample (PG-MF-0089) was deposited at the herbarium of the Pharmacognosy Department, Tanta University, Egypt. The specimens were dried at room temperature for 10 days and then powdered. The powder (350 g) was extracted with 80% methanol (3 L × 3 times) using the cold maceration method to yield 50.3 g of BRFE.

Chemicals

Indomethacin was obtained from Kahira Pharmaceutical & Chemical Industries Co. (Egypt). Other chemicals, including dimethyl sulfoxide (DMSO), resazurin, N-phenyl-1-naphthylamine (NPN), o-nitrophenyl-β-D-galactopyranoside (ONPG), DiBAC4(3), Roswell Park Memorial Institute 1640 (RPMI 1640), fetal bovine serum (FBS), L-glutamine, and penicillin-streptomycin solution, were obtained from Merck (USA).

Animals

In total, 60 Sprague–Dawley rats were acclimatized for 2 weeks in wire cages with free access to water and a regular pellet diet. The rats' starting weight was 230–250 g, and their age was 12 weeks.

LC-MS/MS for Metabolite Profiling

Liquid chromatography–electrospray ionization–tandem mass spectrometry (LC-ESI-MS/MS) analysis was conducted at the Children's Cancer Hospital's Proteomics and Metabolomics Unit (57357). Adopting the criteria described by Attallah et al[20] for high-performance liquid-chromatography separation, a Waters reversed-phase X select HSS T3 column (diameter 2.1 mm, length 150 mm, 2.5µ m), a precolumn (Phenomenex), and in-line filter disks (0.5µ m × 3.0 mm) were used. To identify chemicals, PeakView ™ software was used to compare retention duration and *m*/*z* values obtained by MS/MS^2. The XIC Manager in PeakView™ software was used to calculate peak area values. Extracted ion chromatograms

(XICs) for each targeted analyte were automatically created and compared to a user-defined threshold.[20]

The sample was prepared by macerating *B. rapa* L. flowers powder in mild petroleum ether at room temperature. The powder was extracted with methanol after exhaustion, and then the extract was evaporated under vacuum at 45°C. In a 1 mL solution of deionized water: methanol: acetonitrile (50:25:25), 50 mg of the dry residue was added. The sample was vortexed for 2 min, ultrasonicated for 10 min, and then centrifuged at 1000 rpm in this solvent mixture for another 10 min. The sample solution was diluted with the reconstitution solvent, and 10 µL of it was injected at a concentration of 1 µg/L.

Antibacterial Activity

Bacteria

Four standard bacterial strains, *Shigella dysenteriae* ATCC 13313, *Escherichia coli* ATCC 25922, *Salmonella typhimurium* ATCC14028, and *Staphylococcus aureus* ATCC 29213, were used as test organisms for examination of the antibacterial activity of BRFE. These bacterial strains were acquired from the Pharmaceutical Microbiology Department, Faculty of Pharmacy, Tanta University.

Antibacterial Susceptibility Testing

The disk agar diffusion method was used for preliminary screening of the antibacterial activity of BRFE against the tested isolates[20] using ciprofloxacin as a positive control and DMSO as a negative control.

Minimum inhibitory concentration (MIC) values of BRFE against the tested isolates were determined using resazurin-based broth microdilution assay[21,22] starting with a concentration of 1000 µg/mL. All subsequent microbiological assays were performed before and after treatment of the bacteria with BRFE at 0.5 MIC to maintain bacterial viability.

Bacterial Membrane Permeability Studies

Outer membrane permeability was examined in the tested isolates using NPN.[23] Bacterial suspensions (before and after treatment with BRFE at 0.5 MIC) were mixed with 20 µmol NPN solution and then incubated at 37°C. Fluorescence over time was detected at 340/420 nm using a spectrofluorometer (Shimadzu Corporation, Kyoto, Japan).

Inner membrane permeability was assessed in the tested isolates using ONPG as a substrate to detect the cytoplasmic activity of the enzyme β-galactosidase.[24] Bacterial isolates were overnight grown in Mueller–Hinton broth (MHB) supplemented with 2% lactose and then centrifuged. After washing the pellets, they were resuspended in 0.5% NaCl. Next, 34 mmol ONPG was added to the bacterial suspensions (before and after treatment with BRFE at 0.5 MIC). The optical density (OD) was monitored at 420 nm to assess the ONPG degradation by β-galactosidase.

Impact on the Bacterial Membrane Depolarization

Membrane depolarization was studied in the tested isolates before and after treatment with BRFE at 0.5 MIC using the fluorescent dye DiBAC4(3).[25] This fluorescent compound can enter depolarized cells, where it displays increased fluorescence because it binds to intracellular proteins. After staining the tested isolates with 5 µg/mL of DiBAC4(3), they were examined using a FACSVerse flow cytometer (BD Biosciences, USA).

Immunomodulatory Activity

Isolation of Peripheral Blood Mononuclear Cells

Peripheral blood mononuclear cells (PBMCs) were isolated from the blood of healthy donors using Ficoll density gradient centrifugation. Then, they were cultured in flat-bottom 6-well plates in RPMI 1640 medium supplemented with 2 mM L-glutamine, 10% FBS, and 1% penicillin-streptomycin solution. They were incubated for 24 h at 37°C in a humidified atmosphere containing 5% CO_2.

MTT Cell Viability Assessment

The toxicity of BRFE (concentrations of 3.125, 6.25, 12.5, 25, 50, 100, 200, and 400 µg/mL) on PBMCs was assessed using the MTT viability test.[26] The median inhibitory concentration (IC_{50}) of BRFE against PBMCs was determined. In addition, the immunomodulatory activity of BRFE was tested in lipopolysaccharide (LPS)-stimulated PBMCs at 0.5 IC_{50}.

Quantitative Real-Time PCR

The impact of BRFE on the gene expression of cyclooxygenase-2 (COX-2), inducible nitric oxide synthase (iNOS), interleukin (IL)-6, tumor necrosis factor-alpha (TNF-α), and nuclear factor kappa B (NF-κB) in LPS-stimulated PBMCs was studied.[27] Briefly, 2×10^6 cells/mL of PBMCs were cultured in flat-bottom 6-well plates in RPMI 1640 medium for 24 h and then treated with 100 µL of *Escherichia coli* LPS (20 ng/mL) for 24 h in the presence and absence of BRFE at 0.5 IC_{50}. The impact on the gene expression of COX-2, iNOS, IL-6, TNF-α, and NF-κB was evaluated by quantitative reverse transcription polymerase chain reaction (qRT-PCR; primers

are displayed in Table S1). Total RNA was extracted from PBMCs using the RNeasy mini kit (Qiagen, Hilden, Germany) and then converted to complementary DNA (cDNA) using the SensiFAST™ cDNA kit (Bioline, London, UK). Glyceraldehyde 3-phosphate dehydrogenase (GAPDH) was used as an internal control gene, and the SensiFAST™ SYBR green PCR master mix (Bioline) was used. To calculate the fold-change in the gene expression, we used the $2^{-\Delta\Delta CT}$ method.[28]

In vivo Antiulcer Activity

Ulcer Induction

For ulcer induction, Sprague–Dawley rats were administered a single dose of 100 mg/kg of indomethacin dissolved in distilled water via gavage. Briefly, the 60 rats were randomly divided into 4 groups: group 1 (control, n = 15), group 2 (ulcer group, n = 15), group 3 (150 mg/kg of BRFE, n = 15) and group 4 (300 mg/kg of BRFE, n = 15).

The utilized doses of BRFE were based on previous biological investigations for the same species using different plant organs.[29,30]

Groups 3 and 4 (pretreatment groups) were administered 150 and 300 mg/kg of BRFE, respectively, orally via gavage daily for 10 days. On day 10, before administering indomethacin, all rats were fasted for 24 h and housed in big wire mesh-bottom cages to prevent coprophagia. Water access was also restricted for 2 h. The rats were given 100 mg/kg of indomethacin by single gavage for ulcer induction 1 h after treatment. Groups 1 and 2 (given the vehicle instead of either drug for the first 10 days) were given the vehicle and indomethacin, respectively, at the same time on the final day.

All rats were euthanized using ether, and their stomachs were excised before indomethacin dosage and 4 h after indomethacin/vehicle gavage.

Biochemical Studies

Gastric Glutathione and Malondialdehyde Levels Measurement

To prepare tissue for assaying stomach glutathione (GSH) and malondialdehyde (MDA) levels, 250 mg of stomach tissue was homogenized in 2.5 mL of potassium phosphate buffer (pH 7.4) using a PT 3100 homogenizer (Polytron, Zurich, Switzerland) and centrifuged at 4000 rpm for 15 min at 4°C. The level of decreased GSH in the stomach tissue homogenate was measured colorimetrically using a Biodiagnostics kit (Egypt) according to the manufacturer's instructions.[31] Reduced GSH reduces 5,5-dithiobis 2-nitrobenzoic acid (DTNB) to a yellow product, which was detected at 405 nm using a Unico 2100 spectrophotometer (Phoenix, USA). The GSH levels were displayed as mg/g tissue using the following equation:

$$\text{GSH concentration in tissue} = \left(\frac{\text{A sample} \times 66.66}{\text{Weight tissue used(g)}}\right) \text{mg/g tissue}$$

Colorimetrically, MDA levels in the stomach tissue homogenate were measured using a Biodiagnostics kit (Egypt), as previously described.[32] Thiobarbituric acid interacted with MDA in the sample in an acidic medium at 95°C for 30 min. Then, the absorbance of the formed pink compounds was measured at 534 nm using a Unico 2100 spectrophotometer. MDA levels were expressed as nmol/g using the following equation:

$$= \frac{\text{A sample}}{\text{A standard}} \times \frac{10}{\text{Weight tissue used(g)}} \text{nmol/g}$$

Nitric Oxide Levels Measurement

To assay stomach nitric oxide (NO) levels, 250 mg of stomach tissue was homogenized in 2.5 mL of ice-cold normal saline (0.9%). Then, 1 mL of absolute ethanol was added to 0.5 mL of the homogenate to precipitate proteins, and the sample was centrifuged at 3000 rpm for 10 min at 4°C. The nitrite (an indicator of the original NO present) in the stomach was measured to estimate the amount of NO present. In a nutshell, 500 µL of the homogenate supernatant was combined with an equal amount of VCl_3 and Griess reagent (0.2% naphthyl ethylene-diamine and 2% sulphanilamide in 5% hydrochloric acid). After 30 min of incubation at 37°C, the absorbance of the mixture was measured at 540 nm using a spectrophotometer.[33] The nitrite concentration in the sample was calculated and expressed as nmol NO/g tissue in comparison with sodium nitrite standards.[33]

Determination of Prostaglandin E2

The prostaglandin E2 (PGE2) level in the stomach tissue homogenate supernatant was determined using enzyme-linked immunosorbent assay (ELISA; Mouse PGE2 ELISA Kit NOVA) according to the manufacturer's instructions (Bioneovan Co., China).

qPCR

The relative gene expression of IL-10, glutathione peroxidase (GPx), NF-κB, and myeloperoxidase (MPO) was determined using qRT-PCR, as previously described using the B-actin gene as the control gene. Primer sets for genes were designed using Primer 3 PLUS software (v. 0.4.0; 163 http://frodo.wi.mit.edu/; Table S2).

Histopathological Studies

For histological analysis of the stomach of rats, stomach tissue was preserved in 10% formalin for 24 h, embedded in paraffin blocks, serially sectioned to 5 mm thickness using a RM2135 microtome (Leica, Germany), mounted on glass slides, stained with hematoxylin and eosin, and examined using a light microscope (Labomed, USA).

Institutional Review Board Statement

The study was conducted according to the guidelines approved by the research ethics committee of the Faculty of Pharmacy, Tanta University, for the care and use of laboratory animals (approval code TP/RE/10-21-P-001).

Statistical Analysis

All tests were repeated thrice, and the results are presented as means ± standard deviation using SPSS Statistics version 26 (IBM Corp., USA). Parameters that were acquired from the different tested groups were compared with each other using analysis of variance; $p < 0.001$ was considered statistically significant.

Results

LC-ESI-MS/MS of BRFE

The analysis of BRFE using MS-DIAL in LC-MS/MS (negative- and positive-mode ESI) as a modern analytical technique tentatively identified 57 secondary metabolites. The identified metabolites were classified as anthocyanidin-3-*O*-glycosides, alkaloids, aurone derivative, coumarins, flavonoid aglycone, flavonoid glycoside, phenolic acid, and carboxylic acid. Table 1 shows the results of LC-ESI-MS/MS analysis of BRFE metabolites, and Figure 1 shows the total ion chromatogram of BRFE.

Identification of Simple Phenols and Phenolic Acid Derivatives

Simple phenols are represented by three main classes (hydroxy coumarins, hydroxybenzoic acid, hydroxycinnamic acids) and their corresponding derivatives. Two hydroxyl coumarins were identified in negative ion mode ($[M-H]^-$) as 7-hydroxy-4-methyl coumarin scopoletin and daphnetin at *m/z* 174.95, 177.05, and 193.05, respectively. *p*-Hydroxybenzoic acid was identified in $[M-H]^-$at *m/z* 137, and the identified hydroxycinnamic acids and their derivatives identified were [5, 11, 15, 21, 22, 37]. Caffeic acid was found to be the most abundant hydroxycinnamic acid in the chromatogram in $[M-H]^-$at *m/z* 179, followed by 1-*O*-*β*-D-glucopyranosyl sinapate in $[M-H]^-$at *m/z* 385.

Identification of Flavonoids

Flavonoid glycosides detected in BRFE were tentatively identified as isorhamnetin, baicalein, daidzein, kaempferol, luteolin, naringenin, okanin, and rhoifolin glycosides. The identified compounds in $[M-H]^-$were [10, 12, 13, 16, 17, 23, 26, 27, 29, 33, 35, 36, 42, 43, 44, 45] at *m/z* 445.14, 449.11, 625.12, 609.15, 447.09, 447.07, 593.12, 623.16, 415.13, 447.09, 477.1, 479.12, 431.1, 435.13, 577.15, and 481.10, respectively. Isorhamnetin-3-*O*-glucoside was the major identified compound in $[M-H]^-$according to peak area measurements at *m/z* 477 and MS/MS at *m/z* 315 $[M-H-glc]^-$, 299 $[M-H-glc-H_2O]^-$, and 285 $[M-H-glc-OCH3]^-$(Figure 2A), followed by kaempferol-3-*O*-glucoside, luteolin-3′, and 7-di-*O*-glucoside in the same order. The identified compounds in positive ion mode ($[M+H]^+$) were [14, 24, 41, 43, 45] at *m/z* 627, 425, 479, 435, and 481, respectively. Isorhamnetin-3-*O*-glucoside was the major identified compound in $[M+H]^+$ according to peak area measurements at *m/z* 479 and MS/MS at *m/z* 317 $[M+H-glc]^+$ and 301 $[M+H-glc-H_2O]^+$ (Figure 2C). The flavonoid aglycones were represented by nine compounds: [31, 49, 50, 51] in $[M-H]^-$and [47, 52, 53.54, 55] in $[M+H]^+$. The major aglycones were naringenin, luteolin, and quercetin.

Identification of Anthocyanidin-3-*O*-Glycosides

Tentative identification of anthocyanidin-3-*O*-glycosides in BRFE provided insights into the compounds responsible for the characteristic yellow color of most flowers of the family Brassicaceae. Delphinidin, cyanidin, and petunidin glycosides were the most abundant anthocyanins [18, 19, 28, 48] in $[M+H]^+$ at *m/z* 611, 479, 449, and 933, respectively, and compounds [25, 30] in $[M-H]^-$at *m/z* 609 and 449, respectively, according to peak area measurement of the spectrum. In addition, delphinidin-3-*O*-*β*-glucopyranoside was the major anthocyanidin glycoside detected in $[M-2H]^-$at *m/z* 463.09 with characteristic MS/MS at *m/z* 271 and 301 $[M-2H-glc]^-$ (Figure 2B), followed by cyanidin-3-*O*-(2′′-*O*-*β*-glucopyranosyl-*β*-glucopyranoside) in $[M-2H]^-$at *m/z* 609.15 with characteristic MS/MS at *m/z* 227.03, 255.02, 285.03, 463.08 (Figure 2D). Cyanidin-3,5-di-*O*-glucoside was the major anthocyanidin detected in [M]+ at *m/z* 611.16 with MS/MS at *m/z* 449 [M-glc]+ and 287 [M-glc-glc]+. The

Table 1 Phytochemical Profiling of BRFE by LC-MS/MS Analysis (Negative and Positive Mode ESI)

Peak No.	Identification	RT (Min.)	m/z	Peak Height	Peak Area	Ion Mode	Formula	MS/MS	Ref
1	[a] Succinic acid	1.0788	117.02	41,611.6	572,629.8	$[M-H]^-$	$C_4H_6O_4$	73.02, 99.00	[34]
2	[a] D-(+)-Malic acid	1.0913	133.01	810,402	13,089,116	$[M-H]^-$	$C_4H_6O_5$	71.01, 87.00, 114.63	[35]
3	[a] Maleic acid	1.0951	115	141,150	2,155,713	$[M-H]^-$	$C_4H_4O_4$	71.01	[36]
4	[p.a] p-Hydroxybenzoic acid	1.1412	137.02	4951.78	39,562.14	$[M-H]^-$	$C_7H_6O_3$	73.02, 95.64	[37]
5	[p.a] Caffeic acid	1.2297	179.05	51,602.8	768,577.1	$[M-H]^-$	$C_9H_8O_4$	71.05, 75.00, 161.04	[38]
6	[p.a] Sinapyl aldehyde	1.2391	208.97	50,736	403,100.7	$[M+H]^+$	$C_{11}H_{12}O_4$	104.10, 191.95	[39]
7	[p.a] Sinapoyl malate	1.3058	339.07	45,705.9	428,045.8	$[M-H]^-$	$C_{15}H_{16}O_9$	115.00, 159.02, 223.06	[39]
8	[f.g] Syringetin-3-*O*-galactoside	1.345	507.14	7179.44	46,241.8	$[M-H]^-$	$C_{23}H_{24}O_{13}$	165.03, 299.06, 461.11	[40]
9	[ak] Nicotinic acid	1.7833	122.02	5104.44	41,389.61	$[M-H]^-$	$C_6H_5NO_2$	78.03	[41]
10	[f.g] Baicalein-7-*O*-glucuronide	3.8444	445.14	4576.67	51,547.38	$[M-H]^-$	$C_{21}H_{18}O_{11}$	225.06, 285.100	[42]
11	[p.a] 3-(4-Hydroxy-3-methoxy phenyl) prop-2-enoicacid	4.1608	195.06	2148.33	35,963.14	$[M+H]^+$	$C_{10}H_{10}O_4$	89.03, 149.02, 163.03, 177.05	[43]
12	[f.g] Okanin-4′-*O*-glucoside	4.2895	449.11	3360.78	46,512.64	$[M-H]^-$	$C_{21}H_{22}O_{11}$	167.03, 361.09, 403.19	[44]
13	[f.g] Quercetin-3,4′-*O*-di- β -glucopyranoside	4.5287	625.12	16,840.6	69,874.74	[M-H]-	$C_{27}H_{30}O_{17}$	299.02, 301.031, 463.09	[45]
14	[f.g] Quercetin-3,4′-*O*-di- β -glucopyranoside	4.537	627.15	57,862.4	751,368.8	$[M+H]^+$	$C_{27}H_{30}O_{17}$	127.03, 227.03, 303.04, 465.09	[45]
15	[p.a] 3-(4-Hydroxyphenyl) prop-2-enoic acid	4.8291	165.05	3065.56	44,606.8	$[M+H]^+$	$C_9H_8O_3$	91.01, 119.04	[46]
16	[f.g] Luteolin-3′, 7-di-*O*-glucoside	4.9901	609.15	168,158	1,553,536	$[M-H]^-$	$C_{27}H_{30}O_{16}$	285.04, 299.06, 327.04, 447.09	[47]
17	[f.g] Quercitrin	5.0023	447.09	1373	9518.728	$[M-H]^-$	$C_{21}H_{20}O_{11}$	357.17889:36,447.07562:71	[48]
18	[an] Cyanidin-3, 5-di-*O*-glucoside	5.0564	611.16	62,284.1	621,277.4	$[M]^+$	$C_{27}H_{31}O_{16}$	109.03, 145.04, 287.05, 449.10	[49]
19	[an] Petunidin-3-*O*- β -glucopyranoside	5.2046	479.1	10,728	79,983.64	$[M]^+$	$C_{22}H_{23}O_{12}$	229.03, 285.04, 317.06	[49]
20	[p.a] Rosmarinic acid	5.2738	359.09	5802.67	29,515.36	$[M-H]^-$	$C_{18}H_{16}O_8$	151.04201:71,359.09827:71	[50]

21	[p.a] 3-(4-Hydroxy-3,5-dimethoxyphenyl)-2-propenoic acid	5.3157	225.08	11,596.3	157,515.5	$[M+H]^+$	$C_{11}H_{12}O_5$	119.05, 174.02, 177.02, 207.03	[51]
22	[p.a] 1-*O*- D-glucopyranosyl sinapate	5.4676	385.18	13,682.3	76,078.68	$[M-H]^-$	$C_{17}H_{22}O_{10}$	112.98, 153.09, 223.05	[52]
23	[f.g] Luteolin-7-*O*-glucoside	5.5648	447.07	5537.44	34,358.34	$[M-H]^-$	$C_{21}H_{20}O_{11}$	242.94, 283.03	[53]
24	[f.g] Hyperoside	5.8922	465.1	4772.11	53,492.11	$[M+H]^+$	$C_{21}H_{20}O_{12}$	165.02, 177.06, 285.09, 303.05	[54]
25	[an] Cyanidin-3-*O*-(2"-*O*- β -glucopyranosyl- β -glucopyranoside)	6.0085	609.15	259,006	2,543,264	$[M-2H]^-$	$C_{27}H_{31}O_{16}$	227.03, 255.02, 285.03, 463.08	[49]
26	[f.g] Kaempferol-3-*O*-(6-p-coumaroyl)-glucoside	6.2881	593.12	4087.11	21,694.75	$[M-H]^-$	$C_{30}H_{26}O_{13}$	285.04, 431.14, 477.10, 593.13	[55]
27	[f.g] Kaempferol-7-neohesperidoside	6.3006	593.15	7667.44	84,508.66	$[M-H]^-$	$C_{27}H_{30}O_{15}$	283.04, 315.04, 477.10, 593.13	[55]
28	[an] Cyanidin-3-glucoside	6.4017	449.11	17,978.4	105,474.4	$[M]^+$	$C_{21}H_{21}O_{11}$	85.01, 147.02, 201.02, 287.05	[49]
29	[f.g] Isorhamnetin-3-*O*-rutinoside	6.4247	623.16	25,125.9	303,505.5	$[M-H]^-$	$C_{28}H_{32}O_{16}$	300.04, 315.06,477.09, 623.16	[56]
30	[an] Delphinidin-3-*O*- β -glucopyranoside	6.5616	463.09	375,374	3,329,388	$[M-2H]^-$	$C_{21}H_{21}O_{12}$	271.02,286.93, 301.03, 461.55	[49]
31	[f] Hesperetin	6.6146	301.2	4189.44	19,663.35	$[M-H]^-$	$C_{16}H_{14}O_6$	175.03, 255.23, 301.19	[57]
32	[co] Scopoletin	6.9719	190.95	11,402	48,154.79	$[M-H]^-$	$C_{10}H_8O_4$	117.04, 148.01, 176.008	[58]
33	[f.g] Daidzein-8-C-glucoside	7.0587	415.13	6371	39,787.53	$[M-H]^-$	$C_{21}H_{20}O_9$	207.05, 415.11	[59]
34	[p.a] Chlorogenic acid	7.1565	355.15	29,842.8	382,730.7	$[M+H]^+$	$C_{16}H_{18}O_9$	147.04, 162.06, 323.08	[60]
35	[f.g] Kaempferol-3-*O*-glucoside	7.1817	447.09	758,031	5,389,442	$[M-H]^-$	$C_{21}H_{20}O_{11}$	178.99, 284.02, 357.05	[61]
36	[f.g] Isorhamnetin-3-O-glucoside	7.2792	477.1	3,955,113	20,922,760	$[M-H]^-$	$C_{22}H_{22}O_{12}$	178.88, 285.04, 299.01, 313.55, 315.05	[56]
37	[p.a] 3-(4-hydroxy-3-methoxyphenyl) prop-2-enoicacid	7.4109	195.06	6780.78	70,939.2	$[M+H]^+$	$C_{10}H_{10}O_4$	109.06, 123.03, 149.11, 177.05	[43]
38	[co] Scopoletin	7.4590	193.05	29,861.9	409,660.1	$[M+H]^+$	$C_{10}H_8O_4$	91.04, 121.02, 161.02	[58]

(*Continued*)

https://doi.org/10.2147/JIR.S345780 DovePress

Table 1 (Continued).

Peak No.	Identification	RT (Min.)	m/z	Peak Height	Peak Area	Ion Mode	Formula	MS/MS	Ref
39	[au] Maritimetin-6-*O*-glucoside	7.6828	449.11	211,276	2,097,300	$[M+H]^+$	$C_{21}H_{20}O_{11}$	163.05, 201.06, 241.05, 269.04, 287.05	[62]
41	[f.g] Isorhamnetin-3-*O*-glucoside	7.8179	479.12	1,981,740	24,648,674	$[M+H]^+$	$C_{22}H_{22}O_{12}$	287.03, 299.05,301.03, 317.98	[56]
42	[f.g] Kaempferol-3-*O*-α-L-rhamnoside	7.8462	431.1	12,659.7	140,206.6	$[M-H]^-$	$C_{21}H_{20}O_{10}$	268.03, 285.08	[63]
43	[f.g] Naringenin-7-*O*-glucoside	7.8914	435.13	1898.56	9114.708	$[M+H]^+$	$C_{21}H_{22}O_{10}$	147.04, 153.01,273.07	[64]
44	[f.g] Rhoifolin	8.35	577.15	3264.66	34,088.91	$[M-H]^-$	$C_{27}H_{30}O_{14}$	508.84	[65]
45	[f.g] Gossypin	9.57	481.10	3930.66	50,819.41	$[M+H]^+$	$C_{21}H_{20}O_{13}$	189.11	[66]
46	[f] Quercetin	9.6202	301.04	16,805.9	249,482.8	$[M-H]^-$	$C_{15}H_{10}O_7$	151.00, 178.99	[67]
47	[f] Quercetin	9.7925	303.1	11,709.3	132,976	$[M+H]^+$	$C_{15}H_{10}O_7$	153.00, 181.07	[67]
48	[an] Petunidin-3-*O*-(6″-*O*-(4‴-*O*-E-coum)-α-rhamnopyranosyl-β-glucopyranosyl)-5-*O*-β-glucopyranoside	9.805	933.33	7586.56	81,087.66	$[M]^+$	$C_{43}H_{49}O_{23}$	275.20, 317.06, 771.35, 903.31	[49]
49	[f] Naringenin	10.098	271.06	132,825	2,140,767	$[M-H]^-$	$C_{15}H_{12}O_5$	177.07, 201.05, 253.04	[68]
50	[co] Daphnetin	10.52	177.0549	8722.55	108,885.21	$[M-H]^-$	$C_9H_6O_4$	117.03, 133.02	
51	[f] Luteolin	10.939	285.04	78,611.9	946,757.6	$[M-H]^-$	$C_{15}H_{10}O_6$	171.04, 220.07	[69]
52	[f] 3′-Methoxy-4′,5,7-trihydroxyflavonol	11.14	315.05	268,655	2,243,987	$[M-H]^-$	$C_{16}H_{12}O_7$	225.10, 271.03, 283.02, 300.02	[20]
53	[f] Luteolin	11.401	287.05	16,984.9	139,318.8	$[M+H]^+$	$C_{15}H_{10}O_6$	117.07, 147.04	[69]
54	[f] Myricetin	11.426	319.13	3581.22	34,352.16	$[M+H]^+$	$C_{15}H_{10}O_8$	319.15	[20]
55	[f] 3′-Methoxy-4′,5,7-trihydroxyflavonol	11.605	317.07	55,818.1	301,345.8	$[M+H]^+$	$C_{16}H_{12}O_7$	165.01, 179.02, 271.05, 285.04	[20]
56	[f] (+)-3 3′ 4′ 5 7-Pentahydroxyflavan	16.526	291.19	4260.22	52,578.86	$[M+H]^+$	$C_{15}H_{14}O_6$	123.12, 141.07	[70]
57	[f] 3 3′ 4′ 5-Tetrahydroxy-7-methoxyflavone	20.093	317.12	96,989	983,757.1	$[M+H]^+$	$C_{16}H_{12}O_7$	201.15, 317.11	[70]

Notes: [a]Carboxylic acid, [ak]Alkaloid, [an]Anthocyanidin-3-*O*-glycosides, [au]Aurone derivative, [co]Coumarins, [f]Flavonoid aglycone, [f.g]Flavonoid glycoside, [a]Phenolic acid derivative.

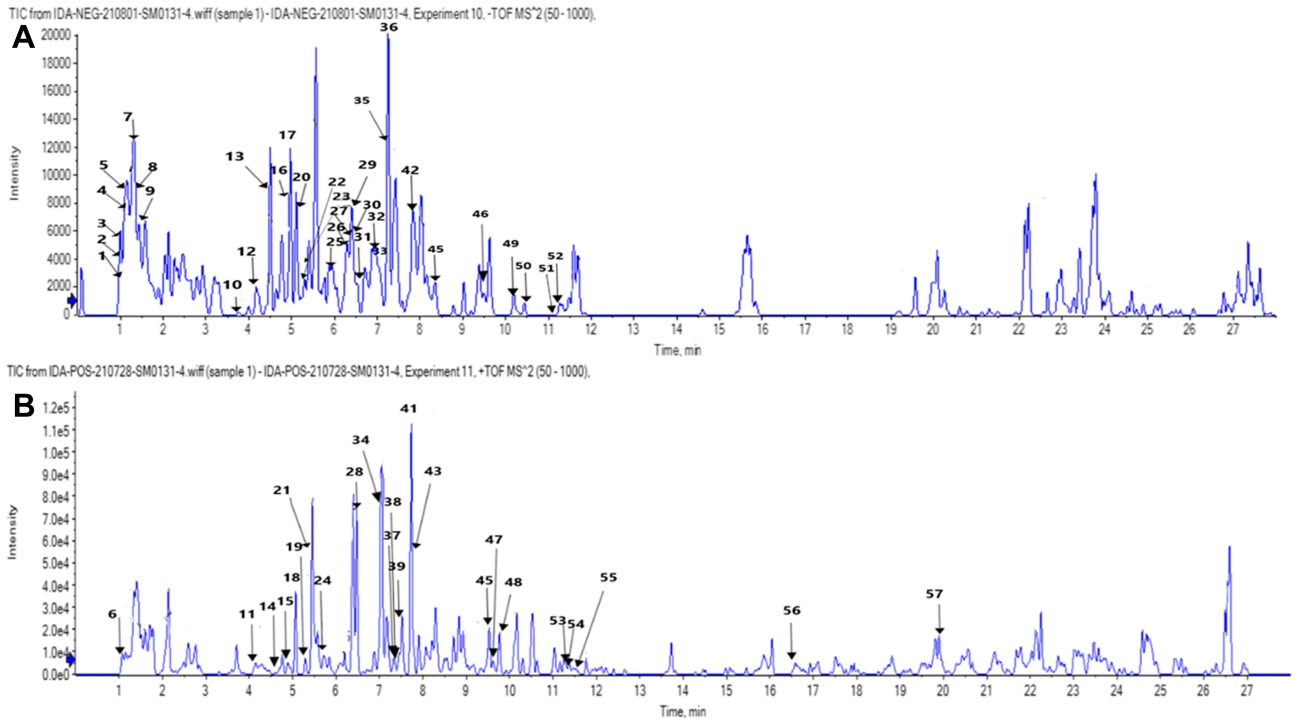

Figure 1 Total ion chromatogram by LC-MS/MS of BRFE labeled with the tentatively identified active metabolites in (**A**) negative ion mode, (**B**) positive ion mode.

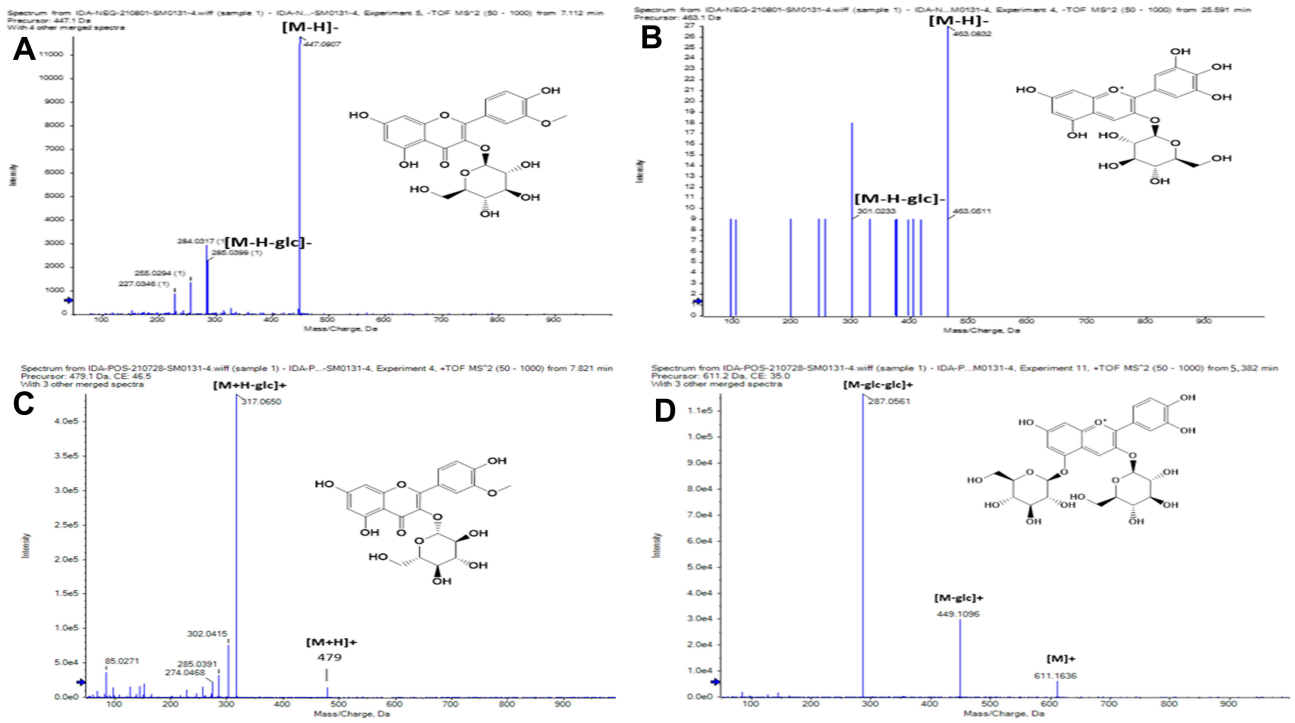

Figure 2 Base peak charts of major identified phenolic compounds of BRFE by LC-ESI-MS/MS in negative ion mode; (**A**) isorhamnetin 3-*O*-glucopyranoside, (**B**) delphinidin-3-*O*-*β*-glucopyranoside, and in positive ion mode; (**C**) isorhamnetin 3-*O*-glucopyranoside, (**D**) cyanidin-3, 5-di-*O*-glucoside.

other identified anthocyanidin 3-*O*-glycosides were cyanidin-3-glucoside, cyanidin-3-*O*-(2''-*O*-*β*-glucopyranosyl-*β*-glucopyranoside), petunidin-3-*O*-*β*-glucopyranoside, and petunidin-3-*O*-(6''-*O*-(4'''-*O*-E-coum)-*α*-rhamnopyranosyl-*β*-glucopyranosyl)-5-*O*-*β*-glucopyranoside trifluoroacetate salt.

Antibacterial Activity

BRFE showed antibacterial activity against the tested isolates, and the MICs are shown in Figure 3. The MICs of ciprofloxacin (positive control) against the tested isolates ranged from 0.125 to 0.5 µg/mL. However, DMSO (negative control) did not exhibit any antimicrobial activity.

Impact on Bacterial Membrane Permeability: Outer Membrane Permeability of Gram-Negative Bacteria

Outer membrane permeability was studied in *S. dysenteriae, E. coli*, and *S. typhimurium* by detection of fluorescent NPN using a spectrofluorophotometer, as the fluorescence of NPN is detectable in the hydrophobic regions of bacteria, such as cell membranes.[23] BRFE (at 0.5 MIC) significantly increased NPN fluorescence, indicating a substantial increase ($p < 0.001$) in the outer membrane permeability, as shown in Figure 4A (a representative example).

Inner Membrane Permeability

If the inner membrane permeability increases, ONPG enters the bacterial cells and is converted by β-galactosidase, which is present in the bacterial cytoplasm, into *O*-nitrophenol (ONP).[24] ONP has a yellow color, and its amount can be detected by measuring the absorbance at OD = 420 over time. An illustrative example is shown in Figure 4B. The inner membrane permeability significantly increased ($p < 0.001$) after BRFE treatment (at 0.5 MIC).

Impact on Bacterial Membrane Depolarization

The impact of BRFE on membrane depolarization of the tested isolates was studied quantitatively using flow cytometry after staining the isolates with DiBAC4(3), a fluorescent compound that can enter depolarized cells and binds to intracellular proteins, resulting in increased fluorescence.[25] BRFE did not produce any significant changes in the membrane depolarization of the tested isolates, and an illustrative example is shown in Figure 5.

Immunomodulatory Activity

MTT Assay

The effect of BRFE (concentrations of 3.125, 6.25, 12.5, 25, 50, 100, 200, and 400 µg/mL) on PBMC viability was evaluated. The IC_{50} against PBMCs was 84.9 ± 0.818 µg/mL, as shown in Figure 6.

qRT-PCR

The relative gene expression of inflammation-related enzymes (COX-2 and iNOS), cytokines (IL-6 and TNF-α), and the transcription factor NF-κB increased in LPS-stimulated PBMCs. Remarkably, treatment of LPS-stimulated PBMCs with BRFE at 0.5 IC_{50} attenuated the upregulation of the gene expression of IL-6 and TNF-α. In addition, it significantly reduced the gene expression of

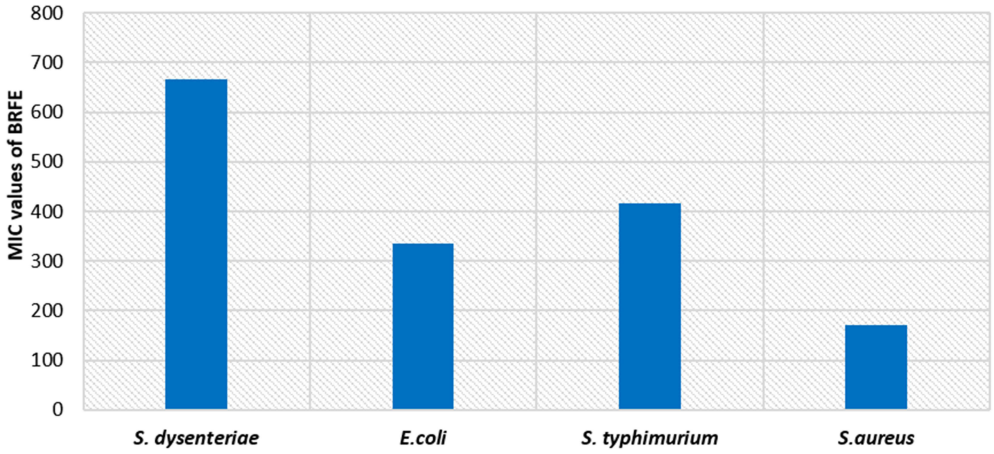

Figure 3 Bar chart showing MIC values of BRFE against the tested bacteria.

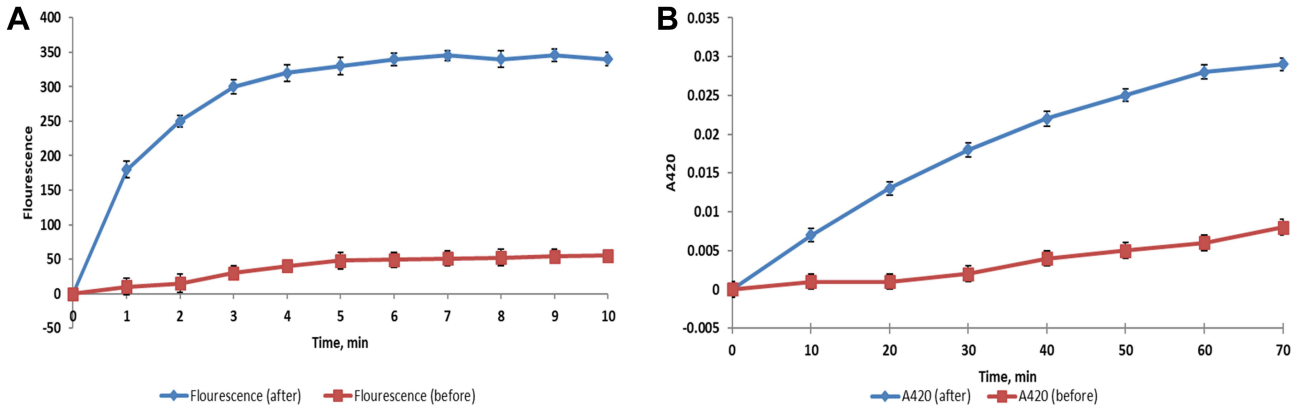

Figure 4 An increase in the (**A**) outer membrane permeability in *E. coli* isolate after treatment with BRFE (125 µg/mL), (**B**) inner membrane permeability in *E. coli* isolate after treatment with BRFE (125 µg/mL).

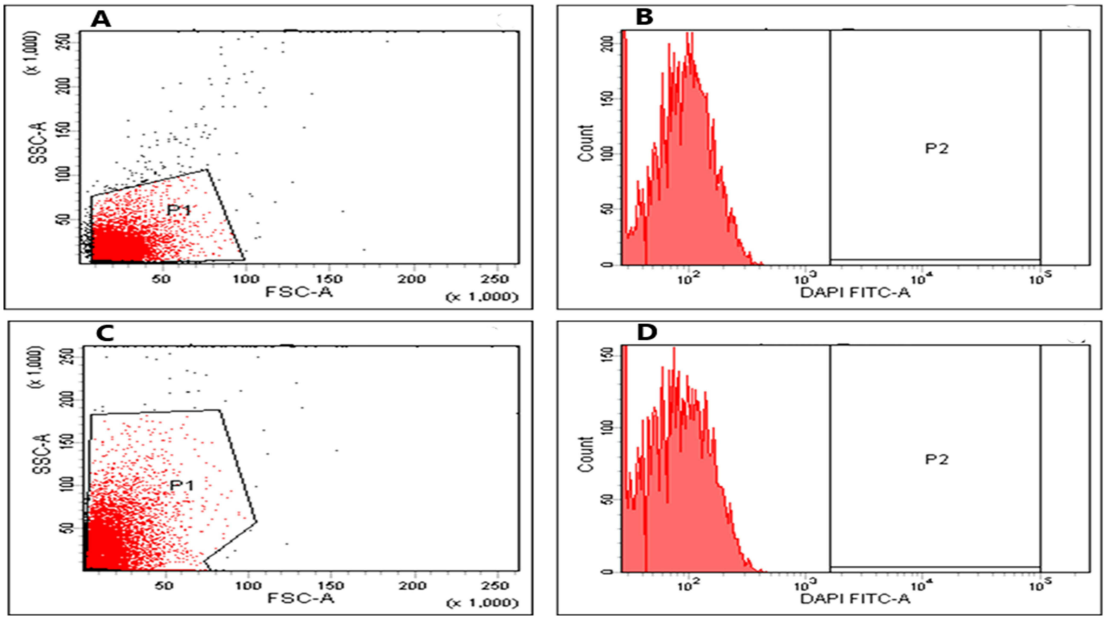

Figure 5 Flow cytometric charts showing fluorescence of *E. coli* isolate (**A**) dot plot and (**B**) histogram, before treatment, and (**C**) dot plot and (**D**) histogram after treatment with BRFE (125 µg/mL).

COX-2, iNOS, and NF-κB ($p < 0.001$) in comparison with the untreated LPS-stimulated PBMCs as shown in Figure 7.

In vivo Studies

Effect on Oxidative Stress Markers

When compared to the control group (group 1), the ulcer group (group 2) had a sharp increase in gastric MDA levels but a significant reduction in gastric GSH levels ($p < 0.001$). Pretreatment with either BRFE (150 or 300 mg/kg: groups 3 and 4, respectively) significantly decreased gastric MDA levels compared with group 2 ($p < 0.001$). A significant increase in gastric GSH levels was observed in both groups 3 and 4 compared with group 2 ($p<0.001$). The results are displayed in Tables S3 and S4 and Figure 8.

Effect on Cytoprotective Mediators

Gastric NO and PGE2 levels significantly reduced in group 2 compared with group 1 ($p < 0.001$). Compared with group 2, groups 3 and 4 exhibited a substantial increase in gastric NO and PGE2 levels ($p < 0.001$). The results are presented in Tables S5 and S6 and Figure 9.

qRT-PCR: Effect on IL-10 Gene Expression

The level of gene expression of IL-10 was 1.25 ± 0.36 in group 1 and 0.75 ± 0.18 in group 2 ($p < 0.001$). Compared

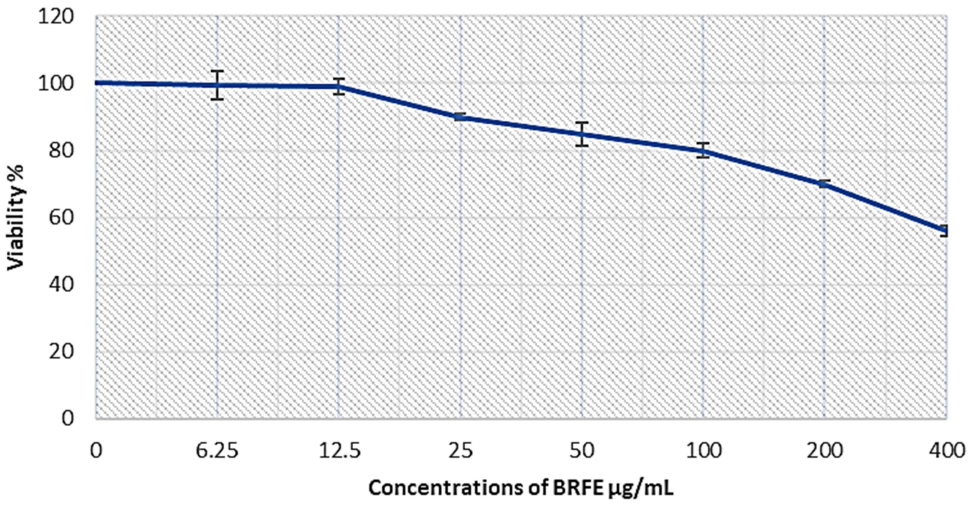

Figure 6 BRFE cytotoxicity on PBMCs using MTT to determine cell viability. IC_{50} was detected in three independent tests.

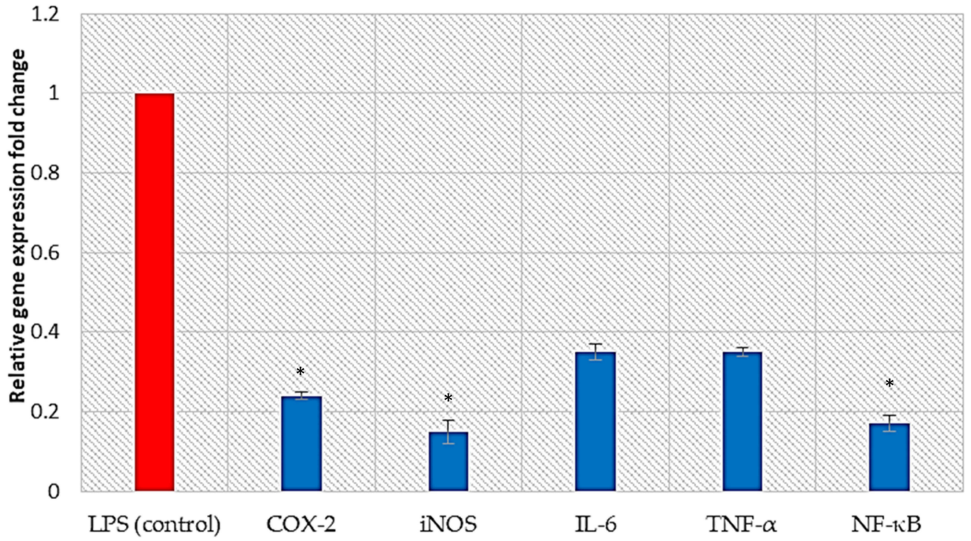

Figure 7 Bar chart showing the effect of BRFE on the gene expression of COX-2, iNOS, IL-6, TNF-α, and NF-κB in LPS-stimulated PBMCs. The symbol * represents a significant change.

with group 2, gene expression of IL-10 significantly increased in both groups 3 and 4 (0.96 ± 0.21 and 1.06 ± 0.2, respectively; $p < 0.001$). There was a significant difference in the gene expression of IL-10 between group 4 and group 1. The results are presented in Table S7 and Figure 10A.

Effect on GPx Gene Expression

The level of gene expression of GPx was 1.34 ± 0.39 in group 1 and 0.75 ± 0.19 in group 2 ($p < 0.001$). When compared with group 2, both groups 3 and 4 showed a marked increase in the gene expression of GPx (1.02 ± 0.22 and 1.2 ± 0.13, respectively; $p < 0.001$). There was a significant difference in the gene expression of GPx between group 4 and group 1. The results are presented in Table S8 and Figure 10B.

Effect on NF-κB Gene Expression

The level of gene expression of NF-κB was 0.81 ± 0.08 in group 1 and 1.75 ± 0.33 in group 2 ($p < 0.001$). Compared with group 2, there was a considerable decrease in the gene expression of NF-κB in both groups 3 and 4 (1.10 ± 0.25 and 0.83 ± 0.10, respectively; $p < 0.001$). There was no notable difference in the gene expression of NF-κB between group 4 and group 1. The results are displayed in Table S9 and Figure 10C.

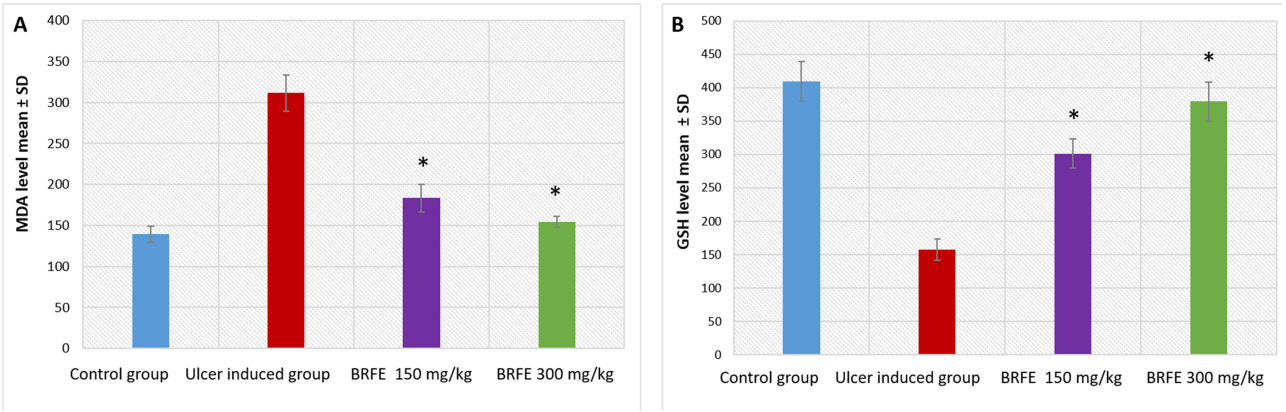

Figure 8 Bar chart showing the effect of BRFE treatment on (**A**) MDA levels and (**B**) GSH levels in the stomach of the tested rats. The symbol * represents a significant change.

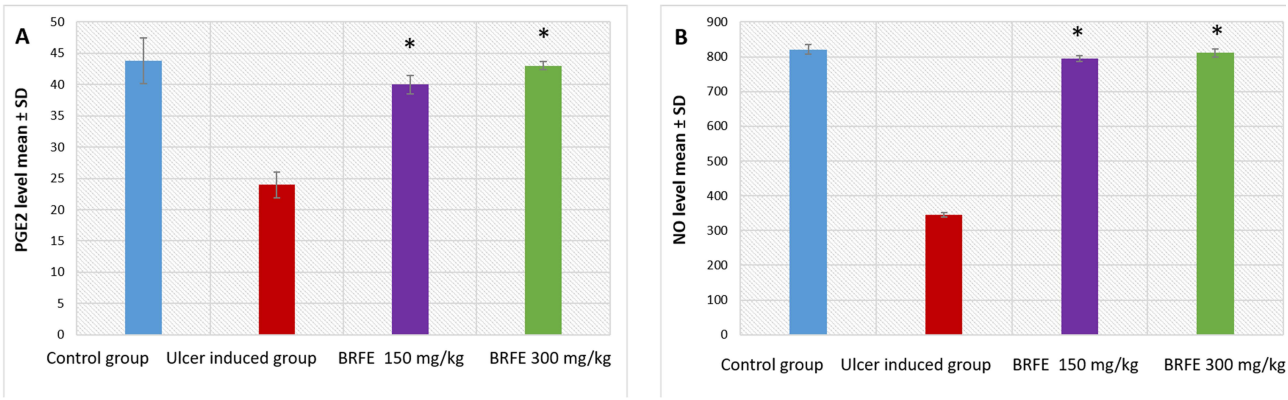

Figure 9 Bar chart showing the effect of BRFE treatment on (**A**) PGE2 levels and (**B**) NO levels in the stomach of the tested rats. The symbol * represents a significant change.

Effect on MPO Gene Expression

The level of gene expression of MPO was 0.81 ± 0.07 in group 1 and 1.86 ± 0.11 in group 2 ($p < 0.001$). Compared with group 2, there was a significant decrease in the gene expression of MPO in both groups 3 and 4 (1.07 ± 0.25 and 0.83 ± 0.10, respectively; $p < 0.001$). There was no substantial difference in the gene expression of MPO between group 4 and group 1 ($p = 0.97$). The results are presented in Table S10 and Figure 10D.

Histopathological Studies

The histopathological results of the examined stomach tissues of groups 3 and 4 showed limited degenerative changes of the gastric mucosa induced by indomethacin compared with the positive control group. The area of mucosal necrosis and ulceration in the positive control group, as a marker of the severity of mucosal and submucosal cellular pathological changes, decreased in group 3. In addition, complete healing of the mucosal tissue was observed in group 4. Moreover, congestion and leukocytic cell infiltration were limited in groups 3 and 4. Mild submucosal edema was observed in group 4, as displayed in Figure 11.

Discussion

BRFE exhibited antibacterial potential against the tested isolates, which cause for GIT infections. *S. dysenteriae* causes bacillary dysentery, which is the main cause of morbidity and mortality among children in many countries.[71] *E. coli* can cause intestinal diseases, especially enterohemorrhagic *E. coli* (EHEC), enteropathogenic *E. coli* (EPEC), enterotoxigenic *E. coli* (ETEC), and enteroinvasive *E. coli* (EIEC).[1] *S. enterica* serovar typhimurium is a common foodborne bacterium that can cause intestinal

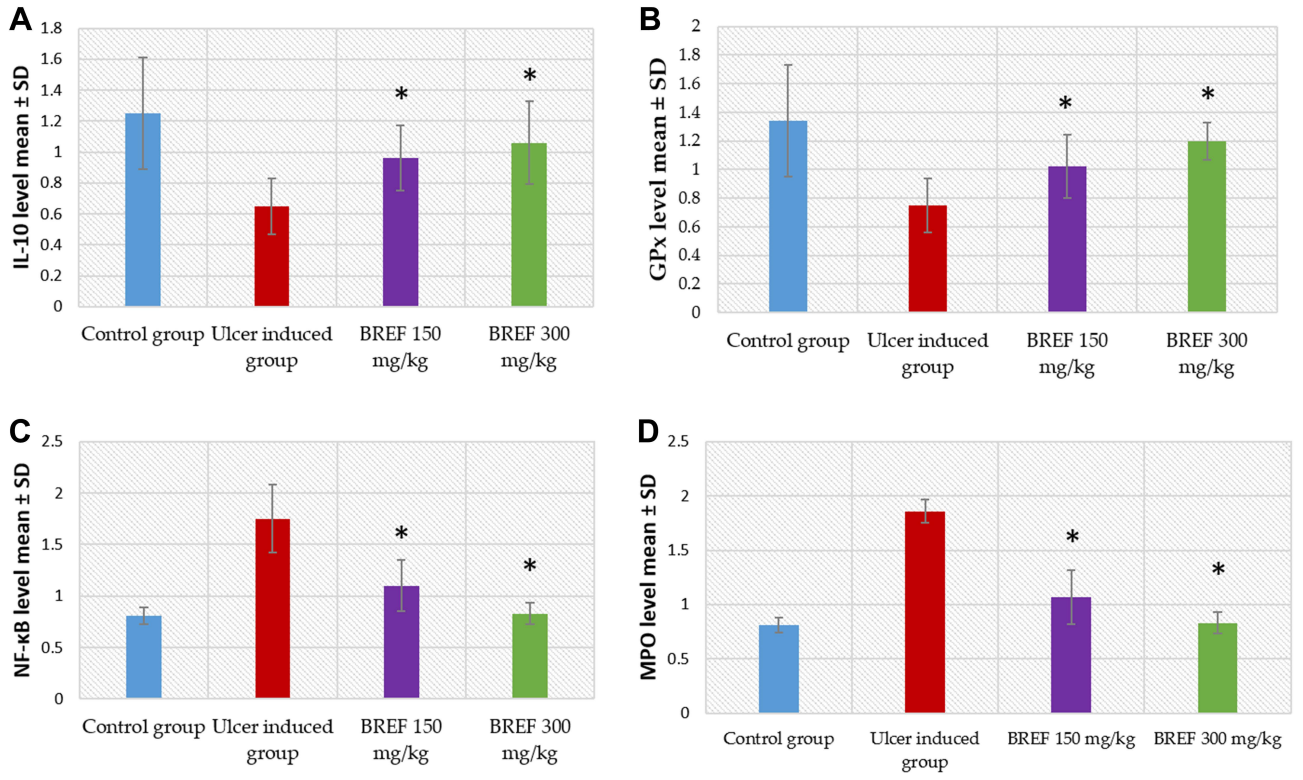

Figure 10 Bar chart showing the level of expressed genes of ulcer treated groups with 150 mg/kg and 300 mg/kg of BRFE compared to control group and ulcer induced group (untreated); (**A**) IL-10 gene, (**B**) GPx gene, (**C**) NF-κB gene and (**D**) MPO gene. The symbol * represents a significant change.

inflammatory diseases and diarrhea; in addition, it results in thousands of deaths worldwide.[72] *S. aureus* can produce staphylococcal enterotoxins that cause food poisoning.[1] For a greater understanding of the antibacterial activity of BRFE, we investigated its impact on the membrane properties of the tested isolates. The outer membrane is present only in Gram-negative bacteria, and it plays an important role in limiting antibiotic access into bacterial cells.[73] BRFE resulted in a substantial increase in the outer membrane permeability in the tested Gram-negative bacteria. The inner membrane is present in both Gram-positive and Gram-negative bacteria. Disrupting the inner membrane by an antimicrobial agent could inhibit many important processes, which would result in a serious assault on bacterial cells.[74] BRFE significantly increased inner membrane permeability in the tested isolates. Membrane potential dissipation is a mechanism of action of many antimicrobial compounds[74]; thus, we investigated the impact of BRFE on the membrane potential of the tested isolates using flow cytometry and found an insignificant change.

PBMCs are blood cells, like lymphocytes and macrophages, having round nuclei. LPS is extracted from the outer membrane of Gram-negative bacteria and is a strong stimulator for macrophages. LPS-stimulated macrophages produce inflammatory mediators, such as prostaglandins and NO, in addition to many inflammatory cytokines, such as IL-6 and TNF-α. Prostaglandins are produced by COX-2 enzyme activity on arachidonic acid, and NO is produced by iNOS activity on the L-arginine amino acid. The production of both prostaglandins and NO are produced by LPS-activated macrophages increases as a result of upregulation of the expression of genes encoding COX-2 and iNOS.[75] Moreover, the NF-κB transcription factor induces pro-inflammatory genes to produce high amounts of pro-inflammatory mediators in LPS-activated macrophages.[76] Overexpression of these bioactive molecules occurs during an inflammatory reaction and could result in detrimental effects on tissues. Hence, inhibition of these interactions offers a good therapeutic effect by decreasing the harmful effects of inflammation, especially GIT inflammatory diseases.[77]

We also investigated the immunomodulatory effect of BRFE on LPS-stimulated PBMCs. After determining the IC_{50} of BRFE against PBMCs, the LPS-stimulated PBMCs were treated with BEFR at 1/2 IC_{50} and the

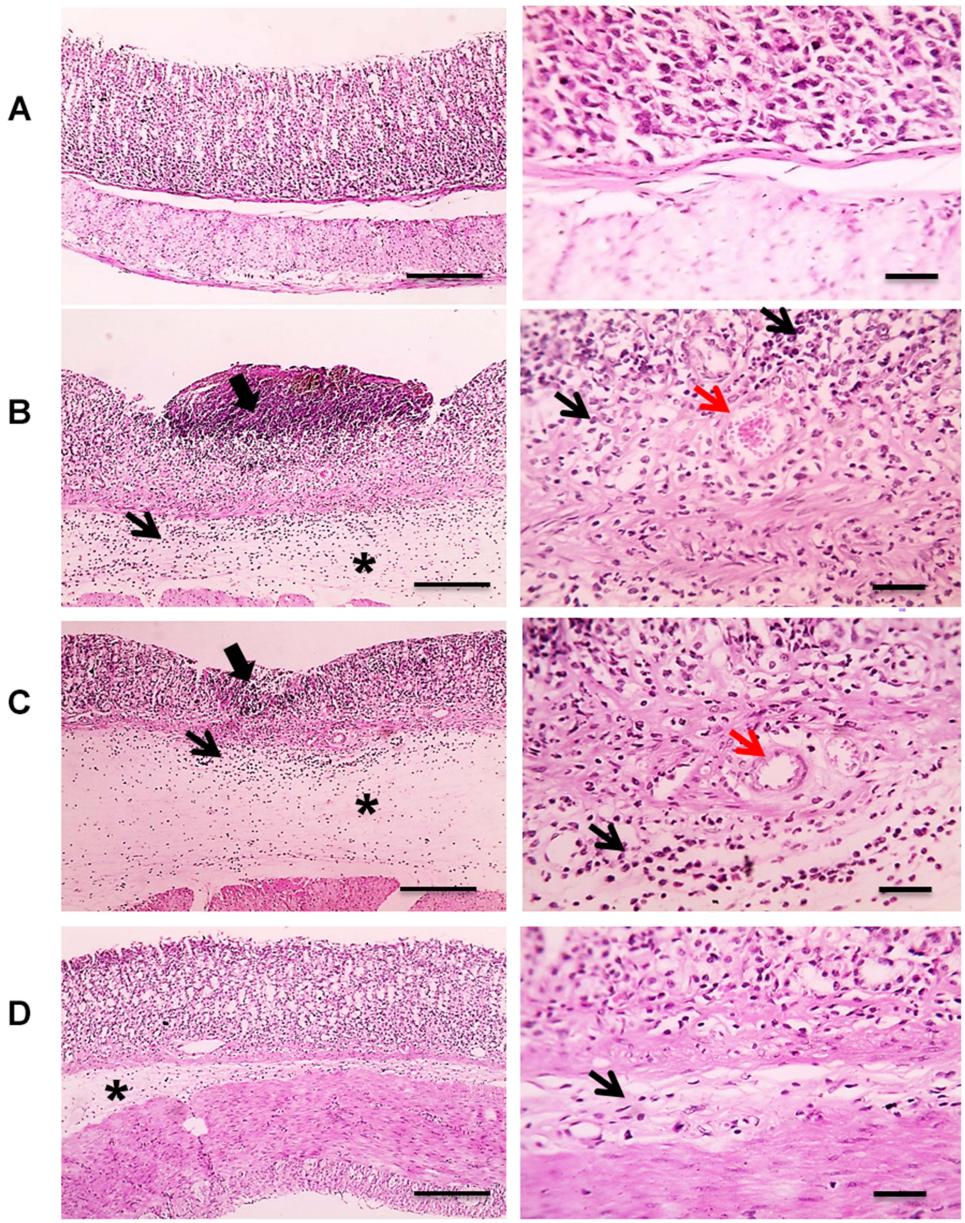

Figure 11 Microscopic pictures of H&E-stained rats' stomachs: (**A**) The control group showing normal glandular gastric mucosa. (**B**) The untreated positive control group induced by indomethacin showing large area of mucosal necrosis and ulceration (thick black arrow) associated with marked submucosal edema (*), congestion (red arrow), and leukocytic cells infiltration (black arrow). (**C**) The treated group with BRFE (150 mg/kg) showing small area of mucosal necrosis and ulceration (thick black arrow) associated with milder submucosal edema (*), congestion (red arrow), and leukocytic cells infiltration (black arrow). (**D**) The treated group with BRFE (300 mg/kg) showing very mild submucosal edema (*) and very few leukocytic cells infiltration (black arrow). The left panel is with low magnification X: 100 bar 100 and the right panel is with high magnification X: 400 bar 50.

relative gene expression of COX-2, iNOS, IL-6, TNF-α, and NF-κB was determined using untreated LPS-stimulated PBMCs as controls. BRFE attenuated the upregulation of the gene expression of COX-2, iNOS, IL-6, TNF-α, and NF-κB.

We aimed to investigate BRFE's gastroprotective efficacy and probable mechanisms of action using an indomethacin-induced gastric ulcer model in rats. Indomethacin was our first choice of drug to be used as it has a higher ulcerogenic potential than other nonsteroidal anti-inflammatory drugs (NSAIDs).[78] BRFE had a dose-dependent effect and provided significant protection against ulcer development. Oral administration of indomethacin causes gastric ulcers in a variety of ways, including suppression of prostaglandin biosynthesis, depletion of gastric mucosal blood flow, and increase in the local inflammatory response, including the over secretion of pro-inflammatory mediators and cytokines, as well as the impairment of local defensive factors.[79]

Neutrophils are innate immune system specialized cells that aid in host defense through phagocytosis and the production of reactive oxygen species (ROS).[80] Neutrophil activation and infiltration in the stomach lead to the creation of lesions. MPO is a heme peroxidase found in neutrophil granules, and its activity reflects the number of neutrophils present in tissues.[81] IN this study, BRFE inhibited neutrophil infiltration in the stomach mucosa by decreasing the activity as well as expression of MPO.

The endogenous antioxidant system of GSH and GPx can be used to scavenge ROS and keep them at healthy levels.[82] As BRFE treatment did not affect other parameters, it only enhanced the activity and gene expression of GPx, an enzyme that functions by oxidizing GSH to glutathione disulfide. This suggests that BRFE has only a minor antioxidant effect.

The main regulator of transcription of numerous genes implicated in inflammation, NF-kB, is activated when ROS is produced. NF-kB is activated during the formation of a stomach ulcer caused by indomethacin, and it promotes the production of inflammatory cytokines such TNF-α, IL-6, and IL-1.[81] Inhibiting NF-kB expression, in addition to making this transcription factor a target for the treatment of inflammatory disorders, is a critical step in preventing stomach ulcer formation.[83]

Our findings showed that BRFE increased the local level of IL-10, but not its expression level, and this is following Basak and Hoffman[84] who found that IL-10 inhibits the synthesis of inflammatory cytokines suppressing the inflammatory response. In our investigation, BRFE partially restored stomach MDA and GSH levels with a significant difference from the control values. By scavenging hydroxyl radicals BRFE has antioxidant properties and inhibits lipid peroxidation[85] and interacting with hypochlorous acid, the most damaging oxidant.[86] Our findings are consistent with El-Ashmawy et al[87] as with a single dose of indomethacin causing a large rise in gastric MDA and a considerable drop in gastric GSH.

PGE2 and NO, two gastroprotective mediators, were shown to be considerably lower in the ulcer group in our investigation. On the contrary, rats treated with BRFE showed a considerable improvement in stomach levels of PGE2 and NO. Reduced PGE2 production and disruption of NO may play a role in the development of gastric ulcers caused by NSAIDs like indomethacin.[88] PGE2 protects the stomach mucosa by boosting mucus secretion, lowering acid secretion, and preserving the blood flow.[89] Due to the vasodilatation function of NO, it can control the stomach pH and increases the blood flow.[90]

In our ulcer model, histopathological analysis of gastric tissue revealed apparent ulcer injury. The results indicated a reduction of pathological degenerative cellular changes of mucosal and submucosal tissues especially at the treatment dose of 300 mg/kg of BRFE. These findings were in line with the considerable increase in stomach levels of the inflammatory mediators (NF-κB and MPO). Different inflammatory mediators are believed to be involved in the pathogenesis of indomethacin-induced stomach ulcers by triggering neutrophil infiltration.[91] The current histopathological findings clarified the gastroprotective effects of BRFE, showing relatively normal mucosa in treated rats.

According to data of LC/MS, it was found that BRFE contained several flavonoids and phenolic compounds as isorhamnetin, luteolin, kaempferol derivatives that were reported to inhibit NO production and explain the anti-inflammatory and gastroprotective effects of BRFE.[92] Luteolin and kaempferol derivatives were reported to have strong inhibitory effects on NO production and these results are consistent with the inhibition of NO in LPS stimulated macrophages.[92,93] Our results also were consistent with previously reported data about the antimicrobial effect of different flavonoids or flavonoid glycosides as quercetin,[94] luteolin,[92,93] isorhamnetin,[95] naringenin,[96] Kaempferol,[97] and anthocyanins derivatives.[98]

Conclusion

In the current investigation, the phytoconstituents of the *B. rapa* flower extract (BRFE) were identified using LC-MS /MS for the first time with identification of 57 compounds. BRFE proved to have antibacterial activity against the pathogenic bacteria that cause GIT infections by increasing the outer and inner membrane permeability. It also showed an immunomodulatory activity on lipopolysaccharide-stimulated peripheral blood mononuclear cells. Moreover, BRFE exhibited an anti-inflammatory activity required for maintaining the gastric mucosa homeostasis in an indomethacin-induced gastric ulcer in rats. Thereby, it could keep the required balance between aggressive and defensive factors in the stomach. Therefore, BRFE could be a future source for novel therapeutic drugs with an activity on the GIT infections as well as the gastric ulcer. Further future studies are recommended to isolate the responsible active ingredients of BRFE that has the main activity on the peptic ulcer. In addition, it is important to formulate BRFE in a pharmaceutical dosage form to maximize the practical incorporation of BRFE in the peptic ulcer treatment regimens.

Supplementary Materials

The following data are available online, Table S1: Sequences of the utilized primers in the immunomodulatory activity, Table S2: Sequences of the utilized primers in the in vivo studies. Table S3: MDA level within the control and the experimental groups, Table S4: GSH level within the control and the experimental groups, Table S5: PGE2 level within the control and the experimental groups, Table S6: Nitric oxide level within the control and the experimental groups, Table S7: IL-10 gene expression within the control and the experimental groups, Table S8: GPX level within the control and the experimental groups, Table S9: NF-KB level within the control and the experimental groups, Table S10: MPO activity within the control and the experimental groups Table S11: B-actin level within the control and the experimental groups.

Acknowledgments

This work was funded by the Deanship of Scientific Research at Princess Nourah bint Abdulrahman University, through the Research Groups Program Grant no. (RGP-1440-0022) (2). The authors, therefore, gratefully acknowledge the DSR technical and financial support.

Funding

This work was funded by the Deanship of Scientific Research at Princess Nourah bint Abdulrahman University, through the Research Groups Program Grant no. (RGP-1440-0022) (2).

Disclosure

The authors report no conflicts of interest in this work.

References

1. Ishaque M, Bibi Y, Ayoubi SA, et al. Iriflophenone-3-C-β-d Glucopyranoside from Dryopteris ramosa (Hope) C. Chr. with Promising Future as Natural Antibiotic for Gastrointestinal Tract Infections. *Antibiotics*. 2021;10(9):1128. doi:10.3390/antibiotics10091128
2. Buddington RK, Kuz'mina V. Digestive system. In: Ostrander GK, editor. *The laboratory fish*. Elsevier; 2000:379–384.
3. Jabri M-A, Marzouki L, Sebai H. Ethnobotanical, phytochemical and therapeutic effects of Myrtus communis L. berries seeds on gastrointestinal tract diseases: a review. *Arch Physiol Biochem*. 2018;124(5):390–396. doi:10.1080/13813455.2017.1423504
4. Dejanovic GM, Asllanaj E, Gamba M, et al. Phytochemical characterization of turnip greens (Brassica rapa ssp. rapa): a systematic review. *PLoS One*. 2021;16(2):e0247032. doi:10.1371/journal.pone.0247032
5. Al Snafi AE. The pharmacological importance of Brassica nigra and Brassica rapa grown in Iraq. *J Pharm Biol*. 2015;5:240.
6. Nawaz H, Shad MA, Muzaffar S. Phytochemical composition and antioxidant potential of Brassica. *Brassica Germplasm Characterization, Breeding Utilization*. 2018;1:7–26.
7. Zhao -C-C, Shen J, Chen J, et al. Phenolic glycoside constituents from Brassica rapa flowers and their α-glucosidase inhibitory activity. *Nat Prod Res*. 2019;33(23):3398–3403. doi:10.1080/14786419.2018.1479704
8. Takahashi Y, Yokoi S, Takahata Y. Genetic divergence of turnip (Brassica rapa L. em. Metzg. subsp. rapa) inferred from simple sequence repeats in chloroplast and nuclear genomes and morphology. *Genetic Resources Crop Evolution*. 2016;63(5):869–879. doi:10.1007/s10722-015-0290-y
9. Gairola S, Sharma J, Bedi YS. A cross-cultural analysis of Jammu, Kashmir and Ladakh (India) medicinal plant use. *J Ethnopharmacol*. 2014;155(2):925–986. doi:10.1016/j.jep.2014.06.029
10. Pierre PS, Jansen JJ, Hordijk CA, Van Dam NM. Differences in volatile profiles of turnip plants subjected to single and dual herbivory above-and belowground. *J Chem Ecol*. 2011;37(4):368–377. doi:10.1007/s10886-011-9934-3
11. Jeong R-H, Wu Q, Cho J-G, et al. Isolation and Identification of Flavonoids from the Roots of Brassica rapa ssp. *J App Biol Chem*. 2013;56(1):23–27. doi:10.3839/jabc.2013.005
12. Cartea ME, Francisco M, Soengas P, Velasco P. Phenolic compounds in Brassica vegetables. *Molecules*. 2011;16(1):251–280. doi:10.3390/molecules16010251
13. Francisco M, Moreno DA, Cartea ME, Ferreres F, García-Viguera C, Velasco P. Simultaneous identification of glucosinolates and phenolic compounds in a representative collection of vegetable Brassica rapa. *J Chromatogr A*. 2009;1216(38):6611–6619. doi:10.1016/j.chroma.2009.07.055
14. Taveira M, Fernandes F, de Pinho PG, Andrade PB, Pereira JA, Valentão P. Evolution of Brassica rapa var. rapa L. volatile composition by HS-SPME and GC/IT-MS. *Microchem Journal*. 2009;93(2):140–146. doi:10.1016/j.microc.2009.05.011
15. Paul S, Geng CA, Yang TH, Yang YP, Chen JJ. Phytochemical and health-beneficial progress of turnip (Brassica rapa). *J Food Sci*. 2019;84(1):19–30. doi:10.1111/1750-3841.14417
16. Bang M-H, Lee D-Y, Oh Y-J, et al. Development of biologically active compounds from edible plant sources XXII. Isolation of indoles from the roots of Brassica campestris ssp rapa and their hACAT inhibitory activity. *App Biol Chem*. 2008;51(1):65–69.
17. Mirzaie H, Johari H, Najafian M, Kargar H. Effect of ethanol extract of root turnip (Brassica rapa) on changes in blood factors HDL, LDL, triglycerides and total cholesterol in hypercholesterolemic rabbits. *Adv Environ Biol*. 2012;25:2796–2812.
18. Oguwike F, Offor C, Nwadighoha A, Ebede S. Evaluation of efficacy of cabbage juice (Brassica oleracea Linne) as potential antiulcer aggent and its effect on the haemostatic mechanism of male albino Wistar rats. *J Dental Med Sci*. 2014;13:92–97.
19. Ryou SH, Cho IJ, Choi B-R, Kim MB, Kwon YS, Ku SK. Brassica oleracea var. capitata L. Alleviates Indomethacin-Induced Acute Gastric Injury by Enhancing Anti-Inflammatory and Antioxidant Activity. *Processes*. 2021;9(2):372. doi:10.3390/pr9020372
20. Attallah NGM, Negm WA, Elekhnawy E, et al. Elucidation of Phytochemical Content of Cupressus macrocarpa Leaves: in Vitro and In Vivo Antibacterial Effect against Methicillin-Resistant Staphylococcus aureus Clinical Isolates. *Antibiotics*. 2021;10(8):890. doi:10.3390/antibiotics10080890
21. Attallah NG, Negm WA, Elekhnawy E, et al. Antibacterial Activity of Boswellia sacra Flueck. Oleoresin Extract against Porphyromonas gingivalis Periodontal Pathogen. *Antibiotics*. 2021;10(7):859. doi:10.3390/antibiotics10070859
22. Wiegand I, Hilpert K, Hancock RE. Agar and broth dilution methods to determine the minimal inhibitory concentration (MIC) of antimicrobial substances. *Nat Protoc*. 2008;3(2):163–175. doi:10.1038/nprot.2007.521

23. Elekhnawy E, Sonbol F, Abdelaziz A, Elbanna T. An investigation of the impact of triclosan adaptation on Proteus mirabilis clinical isolates from an Egyptian university hospital. *Br J Microbiol*. 2021;52:1–11. doi:10.1007/s42770-021-00436-z
24. Negm WA, El-Aasr M, Kamer AA, Elekhnawy E. Investigation of the Antibacterial Activity and Efflux Pump Inhibitory Effect of Cycas thouarsii R. Br. Extract against Klebsiella pneumoniae Clinical Isolates. *Pharmaceuticals*. 2021;14(8):756. doi:10.3390/ph14080756
25. Abdelaziz A, Sonbol F, Elbanna T, El-Ekhnawy E. Exposure to sublethal concentrations of benzalkonium chloride induces antimicrobial resistance and cellular changes in Klebsiellae pneumoniae clinical isolates. *Microbial Drug Resistance*. 2019;25(5):631–638. doi:10.1089/mdr.2018.0235
26. Chan-Zapata I, Canul-Canche J, Fernández-Martín K, et al. Immunomodulatory effects of the methanolic extract from Pouteria campechiana leaves in macrophage functions. *Food Agric Immunol*. 2018;29(1):386–399. doi:10.1080/09540105.2017.1386163
27. Ezzat MI, Hassan M, Abdelhalim MA, El-Desoky AM, Mohamed SO, Ezzat SM. Immunomodulatory effect of Noni fruit and its isolates: insights into cell-mediated immune response and inhibition of LPS-induced THP-1 macrophage inflammation. *Food Funct*. 2021;12(7):3170–3179. doi:10.1039/D0FO03402A
28. Elekhnawy EA, Sonbol FI, Elbanna TE, Abdelaziz AA. Evaluation of the impact of adaptation of Klebsiella pneumoniae clinical isolates to benzalkonium chloride on biofilm formation. *Egypt J Med Human Genetics*. 2021;22(1):1–6. doi:10.1186/s43042-021-00170-z
29. Rahman MS, Jahan N, Rahman SA, Rashid MA. Analgesic and antidepressant activities of Brassica rapa subspecies chinensis (L.) Hanelt on Swiss-albino mice model. *Bangladesh Med Res Counc Bull*. 2015;41(3):114–120. doi:10.3329/bmrcb.v41i3.29886
30. Kim Y-H, Kim Y-W, Oh Y-J, et al. Protective effect of the ethanol extract of the roots of Brassica rapa on cisplatin-induced nephrotoxicity in LLC-PK1 cells and rats. *Biol Pharm Bull*. 2006;29 (12):2436–2441. doi:10.1248/bpb.29.2436
31. Beutler E. Improved method for the determination of blood glutathione. *J Lab Clin Med*. 1963;61:882–888.
32. Kei S. Serum lipid peroxide in cerebrovascular disorders determined by a new colorimetric method. *Clinica chimica acta*. 1978;90 (1):37–43. doi:10.1016/0009-8981(78)90081-5
33. Miranda K, Espey M, Wink D. Unique oxidative mechanisms for the reactive nitrogen oxide species. *Nitric Oxide*. 2001;5:5–62.
34. Jaitz L, Mueller B, Koellensperger G, et al. LC–MS analysis of low molecular weight organic acids derived from root exudation. *Anal Bioanal Chem*. 2011;400(8):2587–2596. doi:10.1007/s00216-010-4090-0
35. Fernández-Fernández R, López-Martínez JC, Romero-González R, Martínez-Vidal JL, Flores MIA, Frenich AG. Simple LC–MS determination of citric and malic acids in fruits and vegetables. *Chromatographia*. 2010;72(1):55–62. doi:10.1365/s10337-010-1611-0
36. Chen H-C, Wu C, Wu K-Y. Determination of the maleic acid in rat urine and serum samples by isotope dilution–liquid chromatography–tandem mass spectrometry with on-line solid phase extraction. *Talanta*. 2015;136:9–14. doi:10.1016/j.talanta.2014.11.021
37. Wang L, Wu Y, Zhang W, Kannan K. Characteristic profiles of urinary p-hydroxybenzoic acid and its esters (parabens) in children and adults from the United States and China. *Environ Sci Technol*. 2013;47(4):2069–2076. doi:10.1021/es304659r
38. Clifford MN, Wu W, Kirkpatrick J, Kuhnert N. Profiling the chlorogenic acids and other caffeic acid derivatives of herbal Chrysanthemum by LC− MS n. *J Agric Food Chem*. 2007;55 (3):929–936. doi:10.1021/jf062314x
39. Sun Y, Wu Y, Zhao Y, Han X, Lou H, Cheng A. Molecular cloning and biochemical characterization of two cinnamyl alcohol dehydrogenases from a liverwort Plagiochasma appendiculatum. *Plant Physiol Biochem*. 2013;70:133–141. doi:10.1016/j.plaphy.2013.05.027
40. Vrhovsek U, Masuero D, Palmieri L, Mattivi F. Identification and quantification of flavonol glycosides in cultivated blueberry cultivars. *J Food Composition Analysis*. 2012;25(1):9–16. doi:10.1016/j.jfca.2011.04.015
41. Lang R, Yagar EF, Eggers R, Hofmann T. Quantitative investigation of trigonelline, nicotinic acid, and nicotinamide in foods, urine, and plasma by means of LC-MS/MS and stable isotope dilution analysis. *J Agric Food Chem*. 2008;56(23):11114–11121. doi:10.1021/jf802838s
42. Yuan Y, Hou W, Tang M, et al. Separation of flavonoids from the leaves of Oroxylum indicum by HSCCC. *Chromatographia*. 2008;68 (11):885–892. doi:10.1365/s10337-008-0859-0
43. Choudhary MI, Begum A, Abbaskhan A, Musharraf SG, Ejaz A. Two new antioxidant phenylpropanoids from Lindelofia stylosa. *Chem Biodivers*. 2008;5(12):2676–2683. doi:10.1002/cbdv.200890221
44. Peng A, Lin L, Zhao M, Sun B. Classification of edible chrysanthemums based on phenolic profiles and mechanisms underlying the protective effects of characteristic phenolics on oxidatively damaged erythrocyte. *Food Res Int*. 2019;123:64–74. doi:10.1016/j.foodres.2019.04.046
45. Venkatalakshmi P, Vadivel V, Brindha P. Identification of Flavonoids in Different Parts of Terminalia catappa L. Using LC-ESI-MS/MS and Investigation of Their Anticancer Effect in EAC Cell Line Model. *J Pharm Sci Res*. 2016;8(4):176.
46. Liu HL, Huang XF, Wan X, Kong LY. Biotransformation of p-Coumaric Acid (=(2E)-3-(4-Hydroxyphenyl) prop-2-enoic Acid) by Momordica charantia Peroxidase. *Helv Chim Acta*. 2007;90 (6):1117–1132. doi:10.1002/hlca.200790111
47. Sofidiya MO, Agunbiade FO, Koorbanally NA, Sowemimo A, Soesan D, Familusi T. Antiulcer activity of the ethanolic extract and ethyl acetate fraction of the leaves of Markhamia tomentosa in rats. *J Ethnopharmacol*. 2014;157:1–6. doi:10.1016/j.jep.2014.09.012
48. Ersoy E, Ozkan EE, Boga M, Yilmaz MA, Mat A. Anti-aging potential and anti-tyrosinase activity of three Hypericum species with focus on phytochemical composition by LC–MS/MS. *Ind Crops Prod*. 2019;141:111735. doi:10.1016/j.indcrop.2019.111735
49. Lee JH, Lee H-J, Choung M-G. Anthocyanin compositions and biological activities from the red petals of Korean edible rose (Rosa hybrida cv. Noblered). *Food Chem*. 2011;129(2):272–278. doi:10.1016/j.foodchem.2011.04.040
50. Elhawary S, Hala E-H, Mokhtar FA, Mansour Sobeh EM, Osman S, El-Raey M. Green Synthesis of Silver Nanoparticles Using Extract of Jasminum officinal L. Leaves and Evaluation of Cytotoxic Activity Towards Bladder (5637) and Breast Cancer (MCF-7) Cell Lines. *Int J Nanomedicine*. 2020;15:9771. doi:10.2147/IJN.S269880
51. Chocholouš P, Vacková J, Šrámková I, Šatínský D, Solich P. Advantages of core–shell particle columns in Sequential Injection Chromatography for determination of phenolic acids. *Talanta*. 2013;103:221–227. doi:10.1016/j.talanta.2012.10.036
52. Glasenapp Y, Cattò C, Villa F, Saracchi M, Cappitelli F, Papenbrock J. Promoting beneficial and inhibiting undesirable biofilm formation with mangrove extracts. *Int J Mol Sci*. 2019;20 (14):3549. doi:10.3390/ijms20143549
53. Mohamed MB, Guasmi F, Ali SB, et al. The LC-MS/MS characterization of phenolic compounds in leaves allows classifying olive cultivars grown in South Tunisia. *Biochem Syst Ecol*. 2018;78:84–90. doi:10.1016/j.bse.2018.04.005
54. Zhou C, Liu Y, Su D, et al. A sensitive LC–MS–MS method for simultaneous quantification of two structural isomers, hyperoside and isoquercitrin: application to pharmacokinetic studies. *Chromatographia*. 2011;73(3–4):353–359. doi:10.1007/s10337-010-1879-0
55. Felipe DF, Brambilla LZ, Porto C, Pilau EJ, Cortez DA. Phytochemical analysis of Pfaffia glomerata inflorescences by LC-ESI-MS/MS. *Molecules*. 2014;19(10):15720–15734. doi:10.3390/molecules191015720

56. Milbury PE, Chen C-Y, Dolnikowski GG, Blumberg JB. Determination of flavonoids and phenolics and their distribution in almonds. *J Agric Food Chem*. 2006;54(14):5027–5033. doi:10.1021/jf0603937
57. Lee J-T, Pao L-H, Hsieh C-D, Huang P-W, Hu OY-P. Development and validation of an LC-MS/MS method for simultaneous quantification of hesperidin and hesperetin in rat plasma for pharmacokinetic studies. *Analytical Methods*. 2017;9(22):3329–3337. doi:10.1039/C7AY00051K
58. Li B, Lu M, Chu Z, et al. Evaluation of pharmacokinetics, bioavailability and urinary excretion of scopolin and its metabolite scopoletin in Sprague Dawley rats by liquid chromatography–tandem mass spectrometry. *Biomed Chromatography*. 2019;33(12):e4678. doi:10.1002/bmc.4678
59. Prasain JK, Jones K, Brissie N, Moore R, Wyss JM, Barnes S. Identification of Puerarin and its metabolites in rats by liquid chromatography− tandem mass spectrometry. *J Agric Food Chem*. 2004;52(12):3708–3712. doi:10.1021/jf040037t
60. Saravanakumar K, Park S, Sathiyaseelan A, et al. Metabolite profiling of methanolic extract of Gardenia jaminoides by LC-MS/MS and GC-MS and its anti-diabetic, and anti-oxidant activities. *Pharmaceuticals*. 2021;14(2):102. doi:10.3390/ph14020102
61. El-Hawary SS, El-Hefnawy HM, El-Raey MA, Mokhtar FA, Osman SM, Jasminum Azoricum L. leaves: HPLC-PDA/MS/MS profiling and in-vitro cytotoxicity supported by molecular docking. *Nat Prod Res*. 2020;1–3. doi:10.1080/14786419.2020.1849203
62. Cojocariu R, Ciobica A, Balmus I-M, et al. Antioxidant capacity and behavioral relevance of a polyphenolic extract of Chrysanthellum americanum in a rat model of irritable bowel syndrome. *Oxid Med Cell Longev*. 2019;2:2019.
63. Cechinel-Zanchett CC, Bolda Mariano LN, Boeing T, et al. Diuretic and renal protective effect of kaempferol 3-O-alpha-l-rhamnoside (afzelin) in normotensive and hypertensive rats. *J Nat Prod*. 2020;83(6):1980–1989. doi:10.1074/jbc.M210328200
64. Kammerer B, Kahlich R, Biegert C, Gleiter CH, Heide L. HPLC-MS/MS analysis of willow bark extracts contained in pharmaceutical preparations. *Phytochemical Analysis*. 2005;16(6):470–478. doi:10.1002/pca.873
65. Liu H, Xu C, Wang W, Zhao Y. Development and validation of an LC-ESI-MS/MS method for simultaneous determination of Ligustroflavone and Rhoifolin in rat plasma and its application to a pharmacokinetic study. *J Chromatogr Sci*. 2017;55(3):267–274. doi:10.1093/chromsci/bmw181
66. Ganapaty S, Chandrashekhar V, Chitme H, Narsu ML. Free radical scavenging activity of gossypin and nevadensin: an in-vitro evaluation. *Indian J Pharmacol*. 2007;39(6):281. doi:10.4103/0253-7613.39147
67. Ferracane R, Graziani G, Gallo M, Fogliano V, Ritieni A. Metabolic profile of the bioactive compounds of burdock (Arctium lappa) seeds, roots and leaves. *J Pharm Biomed Anal*. 2010;51(2):399–404. doi:10.1016/j.jpba.2009.03.018
68. Zhang -T-T. Determination of naringenin and its glucuronic acid conjugate in rat plasma by LC-MS/MS. *Chin Pharm J*. 2014;1:864–868.
69. Keskes H, Belhadj S, Jlail L, et al. LC-MS–MS and GC-MS analyses of biologically active extracts and fractions from Tunisian Juniperus phoenice leaves. *Pharm Biol*. 2017;55(1):88–95. doi:10.1080/13880209.2016.1230139
70. Welch C, Zhen J, Bassène E, Raskin I, Simon JE, Wu Q. Bioactive polyphenols in kinkéliba tea (Combretum micranthum) and their glucose-lowering activities. *J Food Drug Analysis*. 2018;26(2):487–496. doi:10.1016/j.jfda.2017.05.009
71. Khan WA, Griffiths JK, Bennish ML. Gastrointestinal and extra-intestinal manifestations of childhood shigellosis in a region where all four species of Shigella are endemic. *PLoS One*. 2013;8(5):e64097. doi:10.1371/journal.pone.0064097
72. Calo JR, Park SH, Baker CA, Ricke SC. Specificity of Salmonella Typhimurium strain (ATCC 14028) growth responses to Salmonella serovar-generated spent media. *J Environ Sci Health Part B*. 2015;50(6):422–429. doi:10.1080/03601234.2015.1011962
73. Ghai I, Ghai S. Understanding antibiotic resistance via outer membrane permeability. *Infect Drug Resist*. 2018;11:523. doi:10.2147/IDR.S156995
74. Te Winkel JD, Gray DA, Seistrup KH, Hamoen LW, Strahl H. Analysis of antimicrobial-triggered membrane depolarization using voltage sensitive dyes. *Front Cell Dev Biol*. 2016;4:29. doi:10.3389/fcell.2016.00029
75. Viola A, Munari F, Sánchez-Rodríguez R, Scolaro T, Castegna A. The metabolic signature of macrophage responses. *Front Immunol*. 2019;10:1462. doi:10.3389/fimmu.2019.01462
76. Dong J, Li J, Cui L, et al. Cortisol modulates inflammatory responses in LPS-stimulated RAW264. 7 cells via the NF-κB and MAPK pathways. *BMC Vet Res*. 2018;14(1):1–10. doi:10.1186/s12917-018-1360-0
77. Sharifi-Rad M, Anil Kumar NV, Zucca P, et al. Lifestyle, oxidative stress, and antioxidants: back and forth in the pathophysiology of chronic diseases. *Front Physiol*. 2020;11:694. doi:10.3389/fphys.2020.00694
78. Yekta RF, Amiri-Dashatan N, Koushki M, Dadpay M, Goshadrou F, Metabolomic A. Study to Identify Potential Tissue Biomarkers for Indomethacin-Induced Gastric Ulcer in Rats. *Avicenna J Med Biotechnol*. 2019;11(4):299.
79. Hirose H, Takeuchi K, Okabe S. Effect of indomethacin on gastric mucosal blood flow around acetic acid-induced gastric ulcers in rats. *Gastroenterology*. 1991;100(5):1259–1265. doi:10.1016/0016-5085(91)70012-M
80. Glennon-Alty L, Hackett AP, Chapman EA, Wright HL. Neutrophils and redox stress in the pathogenesis of autoimmune disease. *Free Radic Biol Med*. 2018;125:25–35. doi:10.1016/j.freeradbiomed.2018.03.049
81. Antonisamy P, Arasu MV, Dhanasekaran M, et al. Protective effects of trigonelline against indomethacin-induced gastric ulcer in rats and potential underlying mechanisms. *Food Funct*. 2016;7(1):398–408. doi:10.1039/C5FO00403A
82. Halim SZ, Zakaria ZA, Omar MH, Mohtarrudin N, Wahab IRA, Abdullah MNH. Synergistic gastroprotective activity of methanolic extract of a mixture of Melastoma malabathricum and Muntingia calabura leaves in rats. *BMC Complement Altern Med*. 2017;17(1):1–16. doi:10.1186/s12906-017-1992-9
83. Yoo J-H, Lee J-S, Lee Y-S, Ku S, Lee H-J. Protective effect of bovine milk against HCl and ethanol–induced gastric ulcer in mice. *J Dairy Sci*. 2018;101(5):3758–3770. doi:10.3168/jds.2017-13872
84. Basak S, Hoffmann A. Crosstalk via the NF-κB signaling system. *Cytokine Growth Factor Rev*. 2008;19(3–4):187–197. doi:10.1016/j.cytogfr.2008.04.005
85. Biswas K, Bandyopadhyay U, Chattopadhyay I, Varadaraj A, Ali E, Banerjee RK. A novel antioxidant and antiapoptotic role of omeprazole to block gastric ulcer through scavenging of hydroxyl radical. *J Biol Chem*. 2003;278(13):10993–11001.
86. Abdul-Aziz KK. Comparative evaluation of the anti-ulcer activity of curcumin and omeprazole during the acute phase of gastric ulcer. *Food Nut Sci*. 2011;2:628–640.
87. El-Ashmawy NE, Khedr EG, El-Bahrawy HA, Selim HM. Gastroprotective effect of garlic in indomethacin induced gastric ulcer in rats. *Nutrition*. 2016;32(7–8):849–854. doi:10.1016/j.nut.2016.01.010
88. Inas Z, Hala A, Gehan HH. Gastroprotective effect of Cordia myxa L. fruit extract against indomethacin-induced gastric ulceration in rats. *Life Sci J*. 2011;8(3):433–445.
89. Musumba C, Pritchard D, Pirmohamed M. cellular and molecular mechanisms of NSAID-induced peptic ulcers. *Aliment Pharmacol Ther*. 2009;30(6):517–531. doi:10.1111/j.1365-2036.2009.04086.x

90. Morsy MA, Heeba GH, Abdelwahab SA, Rofaeil RR. Protective effects of nebivolol against cold restraint stress-induced gastric ulcer in rats: role of NO, HO-1, and COX-1, 2. *Nitric Oxide*. 2012;27(2):117–122. doi:10.1016/j.niox.2012.06.001
91. Suleyman H, Albayrak A, Bilici M, Cadirci E, Halici Z. Different mechanisms in formation and prevention of indomethacin-induced gastric ulcers. *Inflammation*. 2010;33(4):224–234. doi:10.1007/s10753-009-9176-5
92. Patil KR, Mahajan UB, Unger BS, et al. Animal models of inflammation for screening of anti-inflammatory drugs: implications for the discovery and development of phytopharmaceuticals. *Int J Mol Sci*. 2019;20(18):4367. doi:10.3390/ijms20184367
93. Li Y-C, Yeh C-H, Yang M-L, Kuan Y-H. Luteolin suppresses inflammatory mediator expression by blocking the Akt/NFκB pathway in acute lung injury induced by lipopolysaccharide in mice. *Evid Based Complement Alter Med*. 2012;1;2012.
94. Sholkamy EN, Ahmed MS, Yasser MM, Mostafa AA. Antimicrobial quercetin 3-O-glucoside derivative isolated from Streptomyces antibioticus strain ess_amA8. *J King Saud Univ Sci*. 2020;32(3):1838–1844. doi:10.1016/j.jksus.2020.01.026
95. Ren X, Bao Y, Zhu Y, et al. Isorhamnetin, hispidulin, and cirsimaritin identified in Tamarix ramosissima barks from southern Xinjiang and their antioxidant and antimicrobial activities. *Molecules*. 2019;24(3):390. doi:10.3390/molecules24030390
96. Moon S-H, Lee K-A, Park -K-K, et al. Antimicrobial effects of natural flavonoids and a novel flavonoid, 7-O-Butyl Naringenin, on growth of meat-borne Staphylococcus aureus strains. *Food Sci Animal Resources*. 2011;31(3):413–419. doi:10.5851/kosfa.2011.31.3.413
97. Sati P, Dhyani P, Bhatt ID, Pandey A. Ginkgo biloba flavonoid glycosides in antimicrobial perspective with reference to extraction method. *J Traditional Complement Med*. 2019;9(1):15–23. doi:10.1016/j.jtcme.2017.10.003
98. Ma Y, Ding S, Fei Y, Liu G, Jang H, Fang J. Antimicrobial activity of anthocyanins and catechins against foodborne pathogens Escherichia coli and Salmonella. *Food Control*. 2019;106:106712. doi:10.1016/j.foodcont.2019.106712